

A Primal-Dual Algorithm for Faster Distributionally Robust Optimization

Ronak Mehta¹ Jelena Diakonikolas² Zaid Harchaoui¹

¹University of Washington, Seattle ²University of Wisconsin, Madison

Abstract

We consider the penalized distributionally robust optimization (DRO) problem with a closed, convex uncertainty set, a setting that encompasses the f -DRO, Wasserstein-DRO, and spectral/ L -risk formulations used in practice. We present DRAGO, a stochastic primal-dual algorithm that achieves a state-of-the-art linear convergence rate on strongly convex-strongly concave DRO problems. The method combines both randomized and cyclic components with mini-batching, which effectively handles the unique asymmetric nature of the primal and dual problems in DRO. We support our theoretical results with numerical benchmarks in classification and regression.

1 Introduction

Contemporary machine learning research is fervently exploring the phenomenon of distribution shift, in which predictive models encounter differing data-generating distributions in training versus deployment (Liu et al., 2023; Wiles et al., 2022). An increasingly popular approach for modeling distribution shifts during the training phase is the *distributionally robust optimization (DRO)* problem

$$\min_{w \in \mathcal{W}} \max_{q \in \mathcal{Q}} \left[\mathcal{L}_0(w, q) := \sum_{i=1}^n q_i \ell_i(w) \right], \quad (1)$$

where $w \in \mathcal{W} \subseteq \mathbb{R}^d$ denotes the model weights, $\ell_i : \mathbb{R}^d \rightarrow \mathbb{R}$ denotes the loss on training instance $i \in [n] := \{1, \dots, n\}$, and $q = (q_1, \dots, q_n) \in \mathcal{Q}$ is a probability vector on n atoms. The so-called *ambiguity set* \mathcal{Q} is a collection of potentially unfavorable reweightings arising from modeling possible distributional shifts between train and test data, and is often chosen as a ball about the uniform distribution $\mathbf{1}/n = (1/n, \dots, 1/n)$ in f -divergence (Namkoong and Duchi, 2016; Carmon and Hausler, 2022; Levy et al., 2020) the Wasserstein metric (Esfahani and Kuhn, 2018; Kuhn et al., 2019; Yu et al., 2022), or a spectral/ L -risk set Mehta et al. (2023).

We consider here the penalized version of (1), written

$$\mathcal{L}(w, q) := \sum_{i=1}^n q_i \ell_i(w) - \nu D(q \| \mathbf{1}/n) + \frac{\mu}{2} \|w\|_2^2, \quad (2)$$

where $\mu, \nu \geq 0$ are regularization parameters and $D(q \| \mathbf{1}/n)$ denotes some divergence measure (such as the Kullback-Liebler (KL) or χ^2 -divergence) between the original distribution $\mathbf{1}/n$ and shifted distribution weights q on $[n]$.

Standard (1) and penalized (2) DRO objectives have seen an outpour of recent use in reinforcement learning and control (Lotidis et al., 2023; Yang et al., 2023; Wang et al., 2023a; Yu et al., 2023; Kallus et al., 2022; Liu et al., 2022) as well as creative applications in robotics (Sharma et al., 2020), language modeling (Liu et al., 2021), sparse neural network training (Sapkota et al., 2023), and defense against model extraction (Wang et al., 2023b). However, current optimization algorithms for DRO have limitations in both theory and practice. Some popular algorithms such as SGD have non-vanishing bias, *i.e.*, do not actually converge. Convergence guarantees are often sublinear, in that the required number of calls to first-order (function value-gradient) oracles $\{(\ell_i, \nabla \ell_i)\}_{i=1}^n$ to reach within ε of the minimum of (2) has a polynomial dependence in $1/\varepsilon$ (see Tab. 1). Furthermore, algorithms and analyses tend to focus on specific choices of ambiguity sets (Namkoong and Duchi, 2016; Levy et al., 2020; Mehta et al., 2023).¹

¹See Appx. B for a review of these ambiguity sets, the associated algorithms, and their convergence rates.

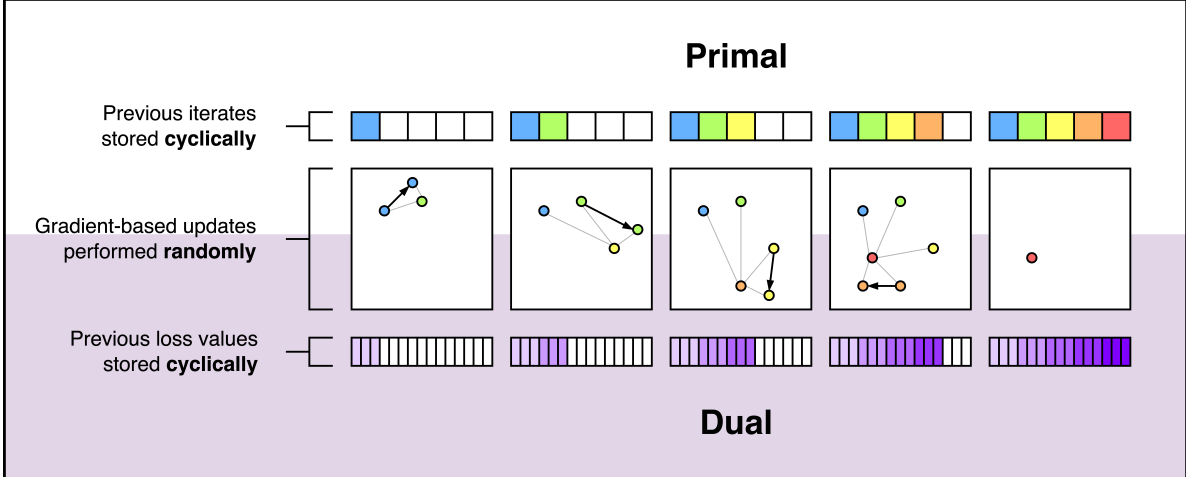


Figure 1: **Conceptual Illustration of DRAGO.** The proposed optimization algorithm combines cyclic and randomized components in the primal and dual updates. A buffer of previous iterates and previous loss values are recorded, where the iterates provide averaging in the primal and the losses provide a variance-reduced gradient estimate in the dual. Stochasticity is used to propose the update directions.

Abstracting to a general optimization viewpoint, both (1) and (2) are coupled min-max problems, with a coupling that is *not bilinear* in general. Such objectives have received much less attention in the optimization literature on primal-dual methods than their bilinearly coupled (i.e., the term in the objective that depends on both w and q is bilinear) counterparts. Many such algorithms employ stochastic *variance-reduced* updates to address possible asymmetry between primal and dual problem constants by using coordinate-style updates in the dual (see Sec. 2). To illustrate the relevance of coordinate updates, observe that the gradient of $q^\top \ell(w)$ with respect to q is $\ell(w)$ itself, immediately costing n first-order oracle evaluations per step. Additionally, the ambiguity set \mathcal{Q} is intrinsically non-separable since all dual solutions must be in the probability simplex, i.e. satisfy $\mathbf{1}^\top q = 1$. This fact, in addition to non-bilinear coupling, presents serious difficulties for the design of such algorithms (Chambolle et al., 2018; Alacaoglu et al., 2020; Song et al., 2021). Given the opportunity within both the DRO and larger optimization community, this paper devises a stochastic algorithm that achieves an unconditional *linear* convergence guarantee while applying to a host of ambiguity sets and penalties.

Contributions We propose DRAGO, a minibatch primal-dual algorithm for the penalized DRO problem (2) that achieves ε -suboptimality in

$$O\left(\left[\frac{n}{b} + \frac{nq_{\max}L}{\mu} + \frac{n}{b}\sqrt{\frac{nG^2}{\mu\nu}}\right] \log\left(\frac{1}{\varepsilon}\right)\right)$$

iterations, where $b \in \{1, \dots, n\}$ is the batch size, $q_{\max} := \max_{q \in \mathcal{Q}, i \in [n]} q_i$ measures the size of the ambiguity set, and G and L are the Lipschitz continuity parameters of ℓ_i and $\nabla \ell_i$, respectively. Theoretically, this is the best-known convergence rate among current penalized DRO algorithms. Practically, DRAGO has a single hyperparameter and operates on any closed, convex ambiguity set for which the map $l \mapsto \arg \max_{q \in \mathcal{Q}} \{q^\top l - \nu D(q \| \mathbf{1}/n)\}$ is computable. DRAGO is also of general conceptual interest as a stochastic variance-reduced primal-dual algorithm for min-max problems. It delicately combines randomized and cyclic components (see Fig. 1), which effectively address the asymmetry of the two problems, as detailed in Sec. 2. The algorithm is explained in Sec. 3, along with its theoretical guarantees. Numerical performance is given in Sec. 4, with concluding remarks in Sec. 5.

Related Work There is a long line of work on variance-reduced algorithms for general stochastic optimization problems (Johnson and Zhang, 2013; Defazio et al., 2014; Palaniappan and Bach, 2016; Cai et al., 2023) and bilinearly coupled min-max problems (Du et al., 2022; Kovalev et al., 2022; Alacaoglu et al., 2022; Song et al., 2021). However, few of these results directly apply to our problem due to the non-bilinearity and non-separability of the dual feasible set. These issues motivated work on reformulating common DRO problems as bilinearly coupled primal-dual prob-

Method	Assumptions	Ambiguity Set	Evaluations of $\{(\ell_i, \nabla \ell_i)\}_{i=1}^n$ Components (Big- \tilde{O})
Sub-Gradient Method	ℓ_i is G -Lipschitz	Any	$n \cdot (GR)^2 \varepsilon^{-2}$
	$\ w - w'\ _2 \leq R$ (if included)	Any	$n \cdot G^2 \mu^{-1} \varepsilon^{-1}$
	$\mu > 0$ (if included)	Any	$n \cdot \mu^{-1} (L + \mu + nG^2/\nu) \log(1/\varepsilon)$
	$\nabla \ell_i$ is L -Lipschitz and $\nu > 0$ (if included)		
$\mathcal{L}_{\text{CVaR-SGD}}$	ℓ_i is G -Lipschitz and in $[0, B]$	θ -CVaR [†]	$\min\{n, B^2 \theta^{-1} \varepsilon^{-2}\} \cdot (GR)^2 \varepsilon^{-2}$
$\mathcal{L}_{\chi^2\text{-SGD}}$	$\ w - w'\ _2 \leq R$ for all $w, w' \in \mathcal{W}$	ρ -ball in χ^2 -divergence [§]	$\min\{n, (1 + \rho)B^2 \varepsilon^{-2}\} \cdot (GR)^2 \varepsilon^{-2}$
$\mathcal{L}_{\chi^2\text{-pen-SGD}}$ (Levy et al., 2020)	$\nu > 0$ (if included)	χ^2 -divergence penalty [§]	$\min\{n, B^2 \nu^{-1} \varepsilon^{-1}\} \cdot (GR)^2 \varepsilon^{-2}$
BROO*	ℓ_i is G -Lipschitz	1-ball in f -divergence	$n \cdot (GR)^{2/3} \varepsilon^{-2/3} + (GR)^2 \varepsilon^{-2}$
BROO*	$\ w - w'\ _2 \leq R$ for all $w, w' \in \mathcal{W}$	1-ball in f -divergence	$n \cdot (GR)^{2/3} \varepsilon^{-2/3} + n^{3/4} (GR \varepsilon^{-1} + L^{1/2} R \varepsilon^{-1/2})$
(Carmon and Hausler, 2022)	$\nabla \ell_i$ is L -Lipschitz (if included)		
SEVR	$\nabla \ell_i$ is L -Lipschitz	Wasserstein-DRO in GLMs	$n \log(1/\varepsilon) + D_{\text{loss}} \varepsilon^{-1} + L^2 D_w^4 \varepsilon^{-2}$
SPPRR	$\ w_0 - w_*\ _2 \leq D_w$	Wasserstein-DRO in GLMs	$(L^2 D_w^2 \varepsilon^{-1} + D_w^2 \varepsilon^{-2}) \log(1/\varepsilon)$
(Yu et al., 2022)	$\max_q \mathcal{L}(w_0, q) - \mathcal{L}(w_*, q_*) \leq D_{\text{loss}}$		
LSVRG	ℓ_i is G -Lipschitz	Spectral Risk Measures (ν small)	None
LSVRG	$\nabla \ell_i$ is L -Lipschitz	Spectral Risk Measures ($\nu \geq \Omega(nG^2/\mu)$)	$(n + nq_{\max} \kappa) \log(1/\varepsilon)$
(Mehta et al., 2023)	$\mu > 0, \nu > 0, \kappa := (L + \mu)/\mu$		
Prospect	ℓ_i is G -Lipschitz	Spectral Risk Measures (ν small)	$n(nq_{\max} \kappa + G^4/(\mu^2 \nu^2) \max\{\kappa^2, G^2/(\mu\nu)\}) \log(1/\varepsilon)$
Prospect	$\nabla \ell_i$ is L -Lipschitz	Spectral Risk Measures ($\nu \geq \Omega(nG^2/\mu)$)	$(n + nq_{\max} \kappa) \log(1/\varepsilon)$
(Mehta et al., 2024)	$\mu > 0, \nu > 0, \kappa := (L + \mu)/\mu$		
DRAGO (Ours)	ℓ_i is G -Lipschitz	Any	$(n + bnq_{\max} L/\mu + n\sqrt{nG^2/(\mu\nu)}) \log(1/\varepsilon)$
	$\nabla \ell_i$ is L -Lipschitz		
	$\mu > 0, \nu > 0, b := \text{Batch Size}$		

Table 1: **Complexity Bounds of DRO Methods.** Oracle complexity (i.e. the number of evaluations of individual components $(\ell_i, \nabla \ell_i)$) required to compute w satisfying $\max_{q \in \mathcal{Q}} \mathcal{L}(w, q) - \mathcal{L}(w_*, q_*) \leq \varepsilon$. Throughout, we assume that each ℓ_i is convex and $\mu, \nu \geq 0$. “Any” ambiguity set refers to all closed, convex sets of probability mass vectors and any 1-strongly convex penalty. *Bounds hold in high probability, as opposed to in expectation. †Examples of spectral risk measures. §Examples of f -divergence.

lems in Song et al. (2022). However, the guarantees obtained in Song et al. (2022) are of the order $O(\varepsilon^{-1})$. On the other hand, algorithms specifically developed for DRO problems typically have only sublinear convergence, as seen in Tab. 1. Indeed, Carmon and Hausler (2022) achieve an upper bound of $O(n\varepsilon^{-2/3} + n\varepsilon^{-1})$ under the f -divergence ball ambiguity set and smooth losses. For the χ^2 -ball and conditional value-at-risk (CVaR) ambiguity set, examples of f -divergences and spectral risk measures, respectively, Levy et al. (2020) achieve upper bounds of $\tilde{O}(\varepsilon^{-3})$ and $\tilde{O}(\varepsilon^{-2})$, for sufficiently small uncertainty sets. The authors also provide an $\Omega(\varepsilon^{-2})$ lower bound for the stochastic first-order oracle model under the CVaR ambiguity set. Mehta et al. (2024) achieve a linear rate $\tau \log(1/\varepsilon)$ with $\tau = n + nq_{\max} (L + \mu)/\mu$, but only when $\nu = \Omega(nG^2/\mu)$ and \mathcal{Q} is a spectral risk measure, and otherwise underperforms the subgradient method (in this case, gradient descent). Notably, when $\nu = \Omega(nG^2/\mu)$, our rate matches the upper bound set by Mehta et al. (2024), but dramatically improves their $O(\text{poly}(n, L/\mu) \ln(1/\varepsilon))$ rate for small ν . LSVRG (Mehta et al., 2023) does not have a guarantee when ν is small.

2 Primal-Dual Asymmetry in Incremental DRO Algorithms

In this section, we elucidate the challenges faced by common incremental algorithms in distributionally robust optimization (DRO) settings and provide intuition about how DRAGO resolves them. We refer to the gradient of the coupled term $q^\top \ell(w)$ of $\mathcal{L}(w, q)$ with respect to w and q as the primal and dual gradients, respectively. Here, *incremental* specifically means that there is a fixed training set which induces n first-order oracles $\{(\ell_i, \nabla \ell_i)\}_{i=1}^n$ (corresponding to loss on individual training examples) and the algorithm makes $O(1)$ calls to them per iteration. This contrasts the *fully stochastic* or *streaming* setting, in which fresh training examples are sampled from the data-generating mechanism at each iteration. This problem setting introduces an asymmetry between the primal and dual problems, as the incremental first-order information provides an additive component $\nabla \ell_i(w)$ of the primal gradient $\frac{1}{n} \sum_{i=1}^n q_i \nabla \ell_i(w)$ but a single coordinate of the dual gradient $\ell(w)$. This phenomenon could, in principle, be handled by designing a

coordinate-style update for the dual variables, such as stochastic Chambolle-Pock-style algorithms (He et al., 2020; Song et al., 2021) in the bilinear setting. Unfortunately, the ambiguity set will always be non-separable due to q being a probability distribution. We argue that respecting this asymmetry while adhering to non-separability is the key ingredient behind the design of DRAGO. In the remainder of this section, we build up to the proposed method by progressive improvements of a standard stochastic primal-dual proximal algorithm. In the following, $c_1, \dots, c_4 > 0$ are constants representing generic algorithmic hyperparameters.

Recall the objective (2). We aim to find saddle-point $(w_*, q_*) \in \mathcal{W} \times \mathcal{Q}$ which satisfies

$$\mathcal{L}(w_*, q) \leq \mathcal{L}(w_*, q_*) \leq \mathcal{L}(w, q_*)$$

for all $(w, q) \in \mathcal{W} \times \mathcal{Q}$. A standard approach to this end is the *primal-dual proximal algorithm* given by the updates

$$w_t := \arg \min_{w \in \mathcal{W}} \left\{ \langle \nabla \ell(w_{t-1})^\top q_{t-1}, w \rangle + \frac{\mu}{2} \|w\|_2^2 + c_1 \frac{\mu}{2} \|w - w_{t-1}\|_2^2 \right\} \quad (3)$$

$$q_t := \arg \max_{q \in \mathcal{Q}} \left\{ \langle \ell(w_t), q \rangle - \nu D(q \| \mathbf{1}_n/n) - c_2 \nu \Delta_D(q, q_{t-1}) \right\}. \quad (4)$$

where $\Delta_D(q, \bar{q})$ denotes the Bregman divergence generated by $q \mapsto D(q \| \mathbf{1}_n/n)$:

$$\Delta_D(q, \bar{q}) = D(q \| \mathbf{1}_n/n) - D(\bar{q} \| \mathbf{1}_n/n) - \langle \nabla D(\bar{q} \| \mathbf{1}_n/n), q - \bar{q} \rangle.$$

In either case, the first term is a linearization of $q^\top \ell(w)$, the second term is a strong convexity or strong concavity term that is retained from the objective, and the final term ensures closeness to the previous iterate via parameters $c_1, c_2 > 0$. In the incremental setting, however, we are unable to observe $\ell(w_t) \in \mathbb{R}^n$ or $\nabla \ell(w_{t-1}) \in \mathbb{R}^{n \times d}$, which are necessary to compute the primal and dual gradients. This leads to the following stochastic variants.

Stochastic Primal-Dual Proximal Method In this algorithm, we replace the gradients $\nabla \ell(w_{t-1})^\top q_{t-1}$ in (3) and $\ell(w_t)$ in (4) with stochastic estimates $q_{t-1, i_t} \nabla \ell_{i_t}(w_{t-1})$ and $\ell_{j_t}(w_t) e_{j_t}$, where e_j is the j -th standard basis vector and (i_t, j_t) are drawn independently and uniformly at random from $[n] := \{1, \dots, n\}$. As stated above, while both stochastic gradient estimates are unbiased, we observe a single additive component of the primal gradient while observing a single coordinate in the dual. In either case, the non-vanishing variance in the gradient estimates prevents convergence in theory and practice, motivating *variance reduction* methods that often have linear convergence guarantees on finite-sum optimization problems.

Incorporating Variance Reduction A common technique for achieving convergent stochastic algorithms is to reduce variance in the gradient estimates using methods from the stochastic simulation literature (Graham and Talay, 2013). Another viewpoint is that these methods pay an additional memory cost to store and recycle past first-order information in order to build a more accurate model of the objective. To be concrete, we describe a variance reduction method inspired by SAGA (Defazio et al., 2014) which is incorporated in DRAGO. Similar methods (Mehta et al., 2023; Yu et al., 2022) are based on the SVRG algorithm (Johnson and Zhang, 2013). We maintain two tables $\hat{\ell}_t \in \mathbb{R}^n$ and $\hat{g}_t \in \mathbb{R}^{n \times d}$, which serve as approximations of the losses and gradients $\ell(w_t)$ and $\nabla \ell(w_{t-1})$, respectively. Using indices (i_t, j_t) , we define the ‘‘adjustment’’ vectors

$$\delta_t^P := n q_{t-1, i_t} \nabla \ell_{i_t}(w_{t-1}) - n q_{t-2, i_t} \hat{g}_{t-2, i_t} \quad \text{and} \quad \delta_t^D := (\ell_{j_t}(w_t) - \hat{\ell}_{t-1, j_t}) e_{j_t}$$

and use the associated gradient estimates

$$v_t^P := \hat{g}_{t-1}^\top q_{t-1} + c_3 \delta_t^P \quad \text{and} \quad v_t^D := \hat{\ell}_t + c_4 \delta_t^D \quad (5)$$

for the primal and dual in (3) and (4), respectively. Typically, the same indices used to define the update would be used to update the tables, in that $g_{t, i_t} \leftarrow \nabla \ell_{i_t}(w_t)$ and $\hat{\ell}_{t, j_t} \leftarrow \ell_{j_t}(w_t)$, resulting in a fully randomized algorithm. Additionally, observe that when changing one element of the gradient table from iteration $t-1$ to t , we would need to recompute $g_{t-1}^\top q_{t-1} = \sum_{i=1}^n g_{t-1, i} q_{t-1, i}$ in (5) on every iteration, costing $O(nd)$ arithmetic operations, as non-separability forces the entire dual vector to change every iteration. As we now demonstrate, this recomputation can be avoided and convergence can be established by employing an algorithm involving both cyclic and random components, laying the groundwork for our method.

From Asymmetry to Variational Compatibility First, we recognize that the expression (5) need not employ the dual variable q_{t-1} itself, but an approximation (say \hat{q}_{t-1}) if the expected value of $\hat{g}_{t-1}^\top \hat{q}_{t-1} - n\hat{q}_{t-2,i_t} \hat{g}_{t-2,i_t}$ remains close to zero. Second, for such an approximation, there is no requirement to be contained in \mathcal{Q} , which means that we may update \hat{q}_{t-1} using coordinate updates, e.g., by setting $\hat{q}_{t,i_t} \leftarrow q_t$ on every iteration. Then, we can update the aggregation $\hat{g}_t^\top \hat{q}_t \leftarrow \hat{g}_{t-1}^\top \hat{q}_{t-1} + q_{t,i_t} \nabla \ell_{i_t}(w_t) - \hat{q}_{t-1,i_t} \hat{g}_{t-1,i_t}$ using only $O(d)$ arithmetic operations in each iteration. While this solves the computational issue, the question of linear convergence still remains.

Owing to the principle of variance reduction, convergence would require establishing control over the random adjustment terms δ_t^P and δ_t^D , that is, by bounding $\mathbb{E}_{i_t} \|\delta_t^P\|_2^2$ and $\mathbb{E}_{j_t} \|\delta_t^D\|_2^2$. We show that careful control of the dual variation (which results from coordinate-wise updates to the loss table) allows us to obtain unconditional linear convergence. Indeed, for the norm of the dual adjustment to decay, we must control the term

$$\mathbb{E}_{j_t} \|\delta_t^D\|_2^2 = \frac{1}{n} \sum_{j=1}^n (\ell_j(w_t) - \hat{\ell}_{t-1,j})^2. \quad (6)$$

Thus, by increasing the strong concavity parameter ν in (4), one can mitigate dependence on the inner product term, which is the exact term that requires estimating $\ell(w_t)$ well.

We now consider a different approach, creating the main building block of DRAGO. Using the Lipschitzness of each ℓ_i , we can control (6) by ensuring that w_t is close to each of the iterates that were used to fill the loss table most recently. Precisely, letting $\pi(t-1, i)$ be the timestep τ used to fill position i in the table $\hat{\ell}_\tau$ on or before time $t-1$, we can incorporate $w_{\pi(t-1, i)}$ for all i elements into the primal update as a regularization term. Because randomized updates can cause any such $w_{\pi(t-1, i)}$ to be arbitrarily far back in time, which would hamper progress of the primal sequence, we also ensure that every iterate used to fill the table is recent. This is accomplished by updating the table *cyclically* at the end of each step. The gradient estimates are still defined using a random index; but with $(\hat{\ell}_t, \hat{g}_t, \hat{q}_t)$ updated in this time-aware fashion, we can apply G -Lipschitz continuity element-wise to conclude that

$$\sum_{j=1}^n (\ell_j(w_t) - \hat{\ell}_{t-1,j})^2 \leq G^2 \sum_{\tau=t-n+1}^{t-1} \|w_t - w_{\tau \vee 0}\|_2^2. \quad (7)$$

Thus, by ensuring that w_{t-1} is close to past iterates, we can control $\mathbb{E}_{j_t} \|\delta_t^D\|_2^2$ by incorporating an averaging with past iterates in the primal update (3) with a learning rate parameter and without having to impose conditions on the parameter ν (see (4)). This effect is an example of primal-dual *variational compatibility*. Owing to the regularization we apply to the primal, we can control the variations in the dual. This relationship between primal and dual variations is key to our convergence analysis. In the next section, we assemble the components derived above into the DRAGO algorithm and prove its convergence guarantees.

3 The DRAGO Algorithm

In this section, we present the **Distributionally Robust Annular Gradient Optimizer** (DRAGO). DRAGO is “annular” in that we propose cyclic coordinate updates in the loss table $\hat{\ell}_t$ described in Sec. 2, providing a worst-case guarantee on the accuracy of the dual variable estimates. In the remainder of the section, we describe the method, its convergence properties, and computational complexity.

Algorithm Description DRAGO builds naturally from the components detailed in Sec. 2 with a minor change: Given block size b , we first partition the data indices into n/b blocks, written $(B_1, \dots, B_{n/b})$ for $B_K = (K-b+1, \dots, Kb)$. We assume for simplicity that b divides n . Then, as opposed to a pair of indices (i_t, j_t) , we sample a pair of blocks (I_t, J_t) from $[n/b]$. The block size parameter in DRAGO allows us to trade off per-iteration complexity with the number of iterations to achieve the best global complexity (see Thm. 1). In addition, we study cases in which $b=1$ and $b=n/d$, both of which are quantities that are known to the user. For this reason, the method has only a single hyperparameter $\eta > 0$, which is interpreted as a learning rate. The full description is given in Algorithm 1.

Given initial point (w_0, q_0) , the method constructs the loss, gradient, and dual approximation tables $\hat{\ell}_0 = \ell(w_0)$, $\hat{g}_0 = \nabla \ell(w_0)$, and $\hat{q}_0 = q_0$ described in the previous section. We also define the constants β_t and $\tilde{\beta}$, which will balance terms in the primal and dual updates.

On each iteration t :

Algorithm 1 Distributionally Robust Annular Gradient Optimizer (DRAGO)

Input: Learning rate parameter $\eta > 0$, batch size $b \in \{1, \dots, n\}$, number of iterations T .

Initialize $w_0 = 0_d$, $q_0 = \mathbf{1}/n$, $\hat{\ell}_0 = \ell(w_0)$, $\hat{g}_0 = \nabla \ell(w_0)$, and $\hat{q}_0 = q_0$.

Partition $[n]$ into $(B_1, \dots, B_{n/b})$ for $B_K = (K - b + 1, \dots, Kb)$.

Set $\bar{\beta} = 1/[16\eta(1 + \eta)(n/b - 1)^2]$ if $n/b > 1$ and 0 otherwise, and $\beta_t = (1 - (1 + \eta)^{1-t})/(\eta(1 + \eta))$ for $t = 1, \dots, T$.

for $t = 1$ **to** T **do**

Sample blocks I_t and J_t uniformly on $[n/b]$, and define $K_t = t \bmod (n/b) + 1$.

Primal Update:

$$\delta_t^P \leftarrow \frac{1}{b} \sum_{i \in B_{I_t}} (q_{t-1, i} \nabla \ell_i(w_{t-1}) - \hat{q}_{t-2, i} \hat{g}_{t-2, i}).$$

$$v_t^P \leftarrow \hat{g}_{t-1}^\top \hat{q}_{t-1} + \frac{n}{1+\eta} \delta_t^P.$$

$$w_t \leftarrow \arg \min_{w \in \mathbb{R}^d} \left\{ \langle v_t^P, w \rangle + (\beta_t - \bar{\beta}) \frac{\mu}{2} \|w - w_{t-1}\|_2^2 + \bar{\beta} \frac{\mu}{2} \sum_{\tau=t-n/b}^{t-2} \|w - w_{\tau \vee 0}\|_2^2 + \frac{\mu}{2} \|w\|_2^2 \right\}.$$

Update Loss and Gradient Table:

Set $(\hat{\ell}_{t,k}, \hat{g}_{t,k})$ to $(\ell_k(w_t), \nabla \ell_k(w_t))$ if $k \in K_t$ or $(\hat{\ell}_{t-1,k}, \hat{g}_{t-1,k})$ if $k \notin K_t$.

Dual Update:

$$\delta_t^D \leftarrow \frac{1}{b} \sum_{j \in B_{J_t}} (\ell_j(w_t) - \hat{\ell}_{t-1, j}) e_j.$$

$$v_t^D \leftarrow \hat{\ell}_t + \frac{n}{1+\eta} \delta_t^D$$

$$q_t \leftarrow \arg \max_{q \in \mathcal{Q}} \left\{ \langle v_t^D, q \rangle - \nu D(q \| \mathbf{1}_n/n) - \beta_t \nu \Delta_D(q, q_{t-1}) \right\}.$$

Update Dual Approximation:

Set $\hat{q}_{t,k}$ to $q_{t,k}$ if $k \in K_t$ or $\hat{q}_{t-1,k}$ if $k \notin K_t$.

end for

return (w_T, q_T) .

1. Sample random block indices (I_t, J_t) from $[n/b]$ and define the cyclic block index K_t .
2. Compute the primal gradient estimate v_t^P using I_t and perform the primal update in line 10.
3. Refresh block K_t of the loss table and gradient table using w_t in line 12.
4. Compute the dual gradient estimate v_t^D using J_t and perform the dual update in line 16.
5. Refresh block K_t of the dual approximation table \hat{q}_t using q_t in line 18.

We highlight two non-standard aspects of Algorithm 1. The primal update incorporates a term $\bar{\beta} \frac{\mu}{2} \sum_{\tau=t-n/b}^{t-2} \|w - w_{\tau \vee 0}\|_2^2$ which ensures that w_t is close to each $w_{t-2}, \dots, w_{t-n/b}$. The constant $\bar{\beta}$ trades off this aspect of the primal update objective with the term $(\beta_t - \bar{\beta}) \frac{\mu}{2} \|w - w_{t-1}\|_2^2$, which ensures proximity to the most recent iterate w_t . Second, the algorithm incorporates both random and cyclic selection of the blocks, by defining $K_t = t \bmod (n/b) + 1$. The random component is useful for having a near-unbiased gradient estimate whereas the cyclic component, as mentioned before, allows us to control the variation of the term δ_t^D in the analysis. We proceed to the theoretical statements.

Convergence Analysis Recall the primal and dual optima w_* and q_* as satisfying $\mathcal{L}(w_*, q) \leq \mathcal{L}(w_*, q_*) \leq \mathcal{L}(w, q_*)$ for any $w \in \mathcal{W}$ and $q \in \mathcal{Q}$. We measure suboptimality by way of the gap function, defined as

$$\gamma_t := \mathcal{L}(w_t, q_*) - \mathcal{L}(w_*, q_t) - \frac{\mu}{2} \|w_t - w_*\|_2^2 - \frac{\nu}{2} \|q_t - q_*\|_2^2.$$

Note that $\gamma_t \geq 0$, as it is the sum of non-negative quantities

$$\mathcal{L}(w_t, q_*) - \mathcal{L}(w_*, q_*) - \frac{\mu}{2} \|w_t - w_*\|_2^2 \geq 0 \text{ and } \mathcal{L}(w_*, q_*) - \mathcal{L}(w_*, q_t) - \frac{\nu}{2} \|q_t - q_*\|_2^2 \geq 0.$$

The main result is presented in Thm. 1, where we define \mathbb{E}_0 to be the expected value taken over the randomness of sampling block indices $\{(I_t, J_t)\}_{t=1}^T$.

Theorem 1. *Define the sequence*

$$a_1 = 1, a_2 = 4\eta, \text{ and } a_t = (1 + \eta) a_{t-1} \text{ for } t > 2,$$

along with its partial sum $A_t = \sum_{\tau=1}^t a_\tau$. There is an absolute constant C such that using the parameter

$$\eta = C \min \left\{ \frac{b}{n}, \frac{\mu}{Lnq_{\max}}, \frac{b}{n} \sqrt{\frac{\mu\nu}{nG^2}} \right\},$$

the iterates of DRAGO satisfy:

$$\sum_{t=1}^T a_t \mathbb{E}_0[\gamma_t] + \frac{A_T \mu}{4} \mathbb{E}_0 \|w_T - w_\star\|_2^2 + \frac{A_T \nu}{4} \mathbb{E}_0 \|q_T - q_\star\|_2^2 \leq \frac{nG^2}{\nu\mu^2} \|\nabla \ell(w_0)^\top q_0\|_2^2.$$

By dividing the result of Thm. 1 by A_T , we see that both the expected gap and expected distance-to-optimum in the primal and dual sequences decay geometrically in T . Because both a_t and A_t grow geometrically, and, as a consequence, are within a factor $O(1/\eta)$ of each other, the gap and distance-to-optimum guarantees apply to both the average iterate and the last one. It follows that we can compute a point (w_T, q_T) achieving a gap no more than ε using

$$O \left(\frac{n}{b} + \frac{Lnq_{\max}}{\mu} + \frac{n}{b} \sqrt{\frac{nG^2}{\mu\nu}} \right) \ln \left(\frac{1}{\varepsilon} \right) \quad (8)$$

steps of Algorithm 1 for all choices of ν .

The proof of Thm. 1 is provided in Appx. C, along with a high-level overview in Appx. C.1 and illustrative technical lemmas contained in Appx. C.2. Our analysis relies on controlling $a_t \gamma_t$ by bounding $a_t \mathcal{L}(w_\star, q_t)$ above and bounding $a_t \mathcal{L}(w_t, q_\star)$ below. Key technical steps occur in the lower bound. We first apply that $w \mapsto a_t q_t^\top \ell(w)$ is convex to produce a linear underestimator of the function supported at w_t , and then apply that w_t is given as the minimizer of a strongly convex function. This yields

$$a_t \mathcal{L}(w_\star, q_t) \geq a_t q_t^\top \ell(w_t) + a_t \langle \nabla \ell(w_t)^\top q_t - v_t^P, w_\star - w_t \rangle \quad (9)$$

$$+ \frac{a_t \bar{\beta} \mu}{2} \sum_{\tau=t-n/b}^{t-2} \|w_t - w_{\tau \vee 0}\|_2^2 \quad (10)$$

+ telescoping and non-positive terms.

Note that the terms above will be negated when combining the upper and lower bounds. The labeled terms are highly relevant in the analysis, with the second being non-standard. By expanding the definition of v_t^P and adding and subtracting w_{t-1} , we write

$$\begin{aligned} a_t \langle \nabla \ell(w_t)^\top q_t - v_t^P, w_\star - w_t \rangle &= a_t \langle \nabla \ell(w_t)^\top q_t - \hat{g}_{t-1}^\top \hat{q}_{t-1}, w_\star - w_t \rangle \\ &\quad + \frac{na_t}{1+\eta} \langle \delta_t^P, w_\star - w_{t-1} \rangle \\ &\quad + \frac{na_t}{1+\eta} \langle \delta_t^P, w_{t-1} - w_t \rangle. \end{aligned}$$

When choosing the learning rate η correctly, the first two terms will telescope in expectation (see Lem. 9). The third term, after applying Young's inequality, requires controlling $\|\delta_t^P\|_2^2$ in expectation, which we dub the ‘‘primal noise bound’’ (Lem. 3). When we combine the upper and lower bounds, we get a similar inner product term $a_t (q_\star - q_t)^\top (\ell(w_t) - v_t^D)$, and mirroring the arguments above, we encounter the term $\|\delta_t^D\|_2^2$ which duly requires a ‘‘dual

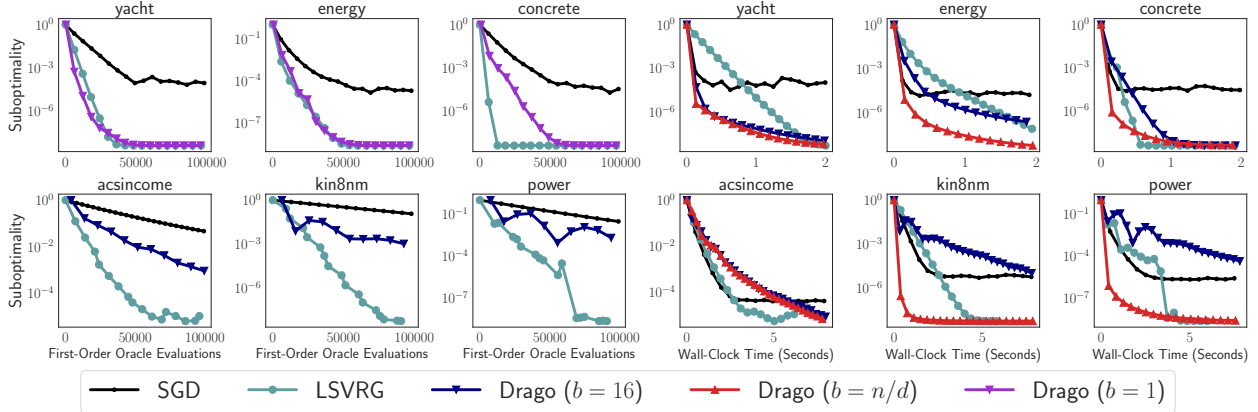


Figure 2: **Regression Benchmarks.** In both panels, the y -axis measure the primal suboptimality gap, defined in (11). Individual plots correspond to particular datasets. **Left:** The x -axis displays the number of individual first-order oracle queries to $\{(\ell_i, \nabla \ell_i)\}_{i=1}^n$. **Right:** The x -axis displays wall-clock time.

noise bound” (Lem. 4). Following (6) and (7) from the previous section that bound is exactly given by

$$\|\delta_t^D\|_2^2 \leq \frac{G^2}{n} \sum_{\tau=t-n/b}^{t-2} \|w_{t-1} - w_{\tau \vee 0}\|_2^2.$$

This will telescope with the second term we introduced in (10), elucidating the importance of this regularization. While the proof is quite technical, this basic idea guides both the analysis and the algorithmic choices we make.

Global Complexity Because our analysis applies to arbitrary batch size b , we can choose the batch size to balance out the computational cost of updating the dual vector q , which is of order- n . Notice that v_t^D can be computed using $O(n)$ operations, so the per-iteration complexity is $O(n + bd)$. Multiplying by (8) and using the nq_{\max} is constant (see Appx. B), we see that the dependence of the global complexity on batch size, sample size, and dimension is $O(n^2/b + nd)$, meaning that batch size $b = n/d$ achieves a global complexity of $O(nd \ln(1/\varepsilon))$ elementary operations to achieve an ε -suboptimality guarantee.

4 Experiments

In this section, we provide numerical benchmarks to measure DRAGO against baselines in terms of evaluations of each component $\{(\ell_i, \nabla \ell_i)\}_{i=1}^n$ and wall clock time. We consider regression and classification tasks. Letting (x_i, y_i) denote a feature-label pair, we have that each ℓ_i represents the squared error loss $\ell_i(w) := \frac{1}{2} (y_i - x_i^\top w)^2$ or multinomial cross-entropy loss $\ell_i(w) := -x_i^\top w_{y_i} + \log \sum_{y \in \mathcal{Y}} \exp(x_i^\top w_y)$, respectively. In the latter case, we denote $w = (w_1, \dots, w_C) \in \mathbb{R}^{C \times d}$, indicating multiclass classification with label set $\mathcal{Y} := \{1, \dots, C\}$. We show results for the conditional value-at-risk (CVaR) (Rockafellar and Royset, 2013) in this section, exploring the effect of sample size n , dimensionality d , and regularization parameter ν on optimization performance. The parameter ν in particular has interpretations both as a conditioning device (as it is inversely related to the smoothness constant of $w \mapsto \max_{q \in \mathcal{Q}} \mathcal{L}(w, q)$) and as a robustness parameter, as it controls the essential size of the ambiguity set.

We compare against baselines that can be used on the CVaR ambiguity set: distributionally robust stochastic gradient descent (SGD) (Levy et al., 2020) and LSVRG (Mehta et al., 2023). For SGD, we use a batch size of 64 and for LSVRG we use the default epoch length of n . For DRAGO, we investigate the variants in which b is set to 1 and $b = n/d$ a priori, as well as cases when b is a tuned hyperparameter. On the y -axis, we plot the primal gap

$$\frac{\max_{q \in \mathcal{Q}} \mathcal{L}(w_t, q) - \mathcal{L}(w_*, q_*)}{\max_{q \in \mathcal{Q}} \mathcal{L}(w_0, q) - \mathcal{L}(w_*, q_*)}, \quad (11)$$

where we approximate $\mathcal{L}(w_*, q_*)$ by running LBFGS (Nocedal and Wright, 1999) on the primal objective until convergence. On the x -axis, we display either the exact number of calls to the first-order oracles of the form $(\ell_i, \nabla \ell_i)$ or the wall clock time in seconds. We fix $\mu = 1$ but vary ν to study its role as a conditioning parameter, which is especially important as prior work establishes different convergence rates for different values of ν (see Tab. 1).

4.1 Regression with Large Block Sizes

In this experiment, we consider six regression datasets, named yacht ($n = 244, d = 6$) (Tsanas and Xifara, 2012), energy ($n = 614, d = 8$) (Baressi Segota et al., 2020), concrete ($n = 824, d = 8$) (Yeh, 2006), acsincome ($n = 4000, d = 202$) (Ding et al., 2021), kin8nm ($n = 6553, d = 8$) (Akujuobi and Zhang, 2017), and power ($n = 7654, d = 4$) (Tüfekci, 2014). In each case, there is a univariate, real-valued output. Notice that most datasets, besides acsincome, are low-dimensional as compared to their sample size. Thus, the default block size n/d becomes relatively large, imposing an expensive per-iteration cost in terms of oracle queries. However, when the block size is high, it also holds that the stochastic gradient estimates in each iteration have lower variance and the table components are updated more frequently, which could improve convergence in principle. The main question of this section is whether DRAGO efficiently manages this trade-off via the block size parameter b . Results for gradient evaluations and wall clock time are given on the left and right panels of Fig. 2, respectively.

Results The DRAGO variant for $b = n/d$ is not included on the left plot, as the number of queries (almost 2,000 in the case of power) penalizes its performance heavily. Still, the same variant performs best or near best on all datasets in terms of wall clock time (right plot). Thus, if the computation of the queries is inexpensive enough, the gains in terms of variance reduction and more recent table elements outweigh the computational cost, and DRAGO can achieve the lowest suboptimality within a fixed time budget. This is most striking in the case of kin8nm, in which DRAGO achieves 10^{-7} primal gap within 1 second, versus LSVRG which is only able to reach within 10^{-2} of the minimum in the same amount of time. We also experiment with tuning b to reach a balance between cost of queries and distance to optimum in the left plot with the $b = 16$ variant. In the datasets with $n \leq 1,000$, DRAGO can match the performance of baselines with only $b = 1$, whereas in the larger datasets, a batch size of 16 is needed to be comparable. The next experiment also supports the use of larger batches in the higher-dimensional, ill-conditioned regime.

4.2 Text Classification Under Ill-Conditioning

We consider a natural language processing example using the emotion dataset (Saravia et al., 2018), which is a classification task consisting of six sentiment categories: sadness, anger, love, fear, joy, and surprise. To featurize the text, we fine-tune a pre-trained BERT network (Devlin et al., 2019) on a held-out set of 8,000 training examples to learn a vectorial representation. We then use a disjoint subset of 8,000 training points and apply PCA to reduce them to 45-dimensional vectors. Because of the six classes this results in $d = 270$ parameters to learn. To study the effect of dual regularization, we consider $\nu \in \{1.0, 0.01, 0.001\}$. As ν decreases, the objective is more poorly conditioned, but the robustness of the learned minimizer may be greater, introducing a key trade-off in constructing DRO objectives which not be considered in generic min-max problems. The results are given in Fig. 3.

Results The run time required for LSVRG to make 500K gradient evaluations is too large to be considered. Furthermore, we observe that LSVRG is vulnerable to ill-conditioned objectives, as it is outperformed by SGD for smaller values of ν in terms of wall clock time. Within 4 seconds, DRAGO can achieve close to a 10^{-5} primal suboptimality gap while the SGD and LSVRG are 2 to 3 orders of magnitude larger in the same amount of time. We hypothesize that because the dual variables in LSVRG are updated once every n iterations, the primal gradient estimates may accrue excessive bias. DRAGO with $b = n/d$, making approximately 30 individual first-order queries per iteration, is performant in terms of oracle queries and wall clock time even as the dual regularization drops 3 orders of magnitude.

5 Discussion

We proposed DRAGO, a stochastic primal-dual algorithm for solving a host of distributionally robust optimization (DRO) problems. The method achieves linear convergence without placing conditions on the dual regularizer, and its empirical performance remains strong across varying settings of the sample size n , dimension d , and the dual

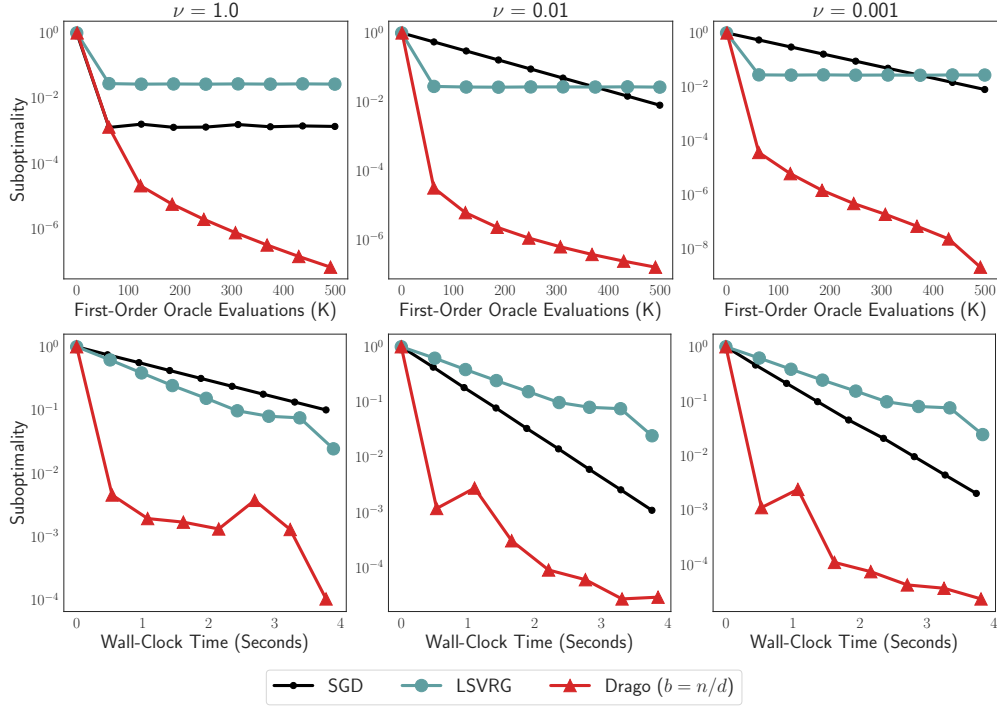


Figure 3: **Text Classification Benchmarks.** In both rows, the y -axis measure the primal suboptimality gap, defined in (11). Columns represent a varying dual regularization parameter ν . The objective becomes ill-conditioned as ν decreases. **Top:** The x -axis displays the number of individual first-order oracle queries to $\{(\ell_i, \nabla \ell_i)\}_{i=1}^n$. **Bottom:** The x -axis displays wall-clock time.

regularization parameter ν . The method combines ideas of variance reduction, mini-batching, and cyclic coordinate-style updates even though the dual feasible set (a.k.a. the ambiguity set) is non-separable. Opportunities for future work include extensions to non-convex settings and applications to min-max problems beyond distributional robustness, such as missing data imputation and fully composite optimization.

Acknowledgements. This work was supported by NSF DMS-2023166, CCF-2019844, DMS-2134012, NIH, ODNI’s IARPA program via 2022-22072200003, U. S. Office of Naval Research under award number N00014-22-1-2348. Part of this work was done while Z. Harchaoui was visiting the Simons Institute for the Theory of Computing. The views and conclusions contained herein are those of the authors and should not be interpreted as representing the official views of ODNI, IARPA, or the U.S. Government.

References

- U. Akujobi and X. Zhang. Delve: A Dataset-Driven Scholarly Search and Analysis System. *SIGKDD Explor. Newsl.*, 19, 2017.
- A. Alacaoglu, O. Fercoq, and V. Cevher. Random extrapolation for primal-dual coordinate descent. In *Proc. ICML'20*, 2020.
- A. Alacaoglu, V. Cevher, and S. J. Wright. On the complexity of a practical primal-dual coordinate method. *arXiv preprint arXiv:2201.07684*, 2022.
- S. Baressi Segota, N. Andelic, J. Kudlacek, and R. Cep. Artificial Neural Network for Predicting Values of Residuary Resistance per Unit Weight of Displacement. *Journal of Maritime & Transportation Science*, 57, 2020.
- J. Blanchet, Y. Kang, and K. Murthy. Robust Wasserstein Profile Inference and Applications to Machine Learning. *Journal of Applied Probability*, 56, 2019.
- X. Cai, C. Song, S. Wright, and J. Diakonikolas. Cyclic Block Coordinate Descent With Variance Reduction for Composite Nonconvex Optimization. In *ICML*, 2023.
- Y. Carmon and D. Hausler. Distributionally Robust Optimization via Ball Oracle Acceleration. In *NeurIPS*, 2022.
- A. Chambolle, M. J. Ehrhardt, P. Richtárik, and C.-B. Schonlieb. Stochastic primal-dual hybrid gradient algorithm with arbitrary sampling and imaging applications. *SIAM Journal on Optimization*, 28(4):2783–2808, 2018.
- L. Condat. Fast projection onto the simplex and the ℓ_1 -ball. *Mathematical Programming*, 2016.
- A. Defazio, F. Bach, and S. Lacoste-Julien. SAGA: A Fast Incremental Gradient Method With Support for Non-Strongly Convex Composite Objectives. *NeurIPS*, 27, 2014.
- J. Devlin, M.-W. Chang, K. Lee, and K. Toutanova. BERT: Pre-training of deep bidirectional transformers for language understanding. In *Proceedings of the 2019 Conference of the North American Chapter of the Association for Computational Linguistics: Human Language Technologies*, 2019.
- F. Ding, M. Hardt, J. Miller, and L. Schmidt. Retiring Adult: New Datasets for Fair Machine Learning. In *NeurIPS*, volume 34. Curran Associates, Inc., 2021.
- S. S. Du, G. Gidel, M. I. Jordan, and C. J. Li. Optimal Extragradient-Based Bilinearly-Coupled Saddle-Point Optimization, 2022.
- P. M. Esfahani and D. Kuhn. Data-driven Distributionally Robust Optimization using the Wasserstein Metric: Performance Guarantees and Tractable Reformulations. *Mathematical Programming*, 171, 2018.
- C. Graham and D. Talay. *Stochastic Simulation and Monte Carlo Methods*. Springer Berlin, Heidelberg, 2013.
- N. He, Z. Harchaoui, Y. Wang, and L. Song. Point process estimation with mirror prox algorithms. *Applied Mathematics & Optimization*, 82:919–947, 2020.
- R. Johnson and T. Zhang. Accelerating Stochastic Gradient Descent using Predictive Variance Reduction. In *NeurIPS*, volume 26, 2013.
- N. Kallus, X. Mao, K. Wang, and Z. Zhou. Doubly Robust Distributionally Robust Off-Policy Evaluation and Learning. In *ICML*, 2022.
- D. Kovalev, A. Gasnikov, and P. Richtárik. Accelerated Primal-Dual Gradient Method for Smooth and Convex-Concave Saddle-Point Problems with Bilinear Coupling. In *NeurIPS*, 2022.
- D. Kuhn, P. M. Esfahani, V. A. Nguyen, and S. Shafieezadeh-Abadeh. Wasserstein Distributionally Robust optimization: Theory and Applications in Machine Learning. *Operations research & management science in the age of analytics*, 2019.

- D. Levy, Y. Carmon, J. Duchi, and A. Sidford. Large-Scale Methods for Distributionally Robust Optimization. In *NeurIPS*, 2020.
- C. J. Li, A. Yuan, G. Gidel, Q. Gu, and M. I. Jordan. Nesterov meets optimism: rate-optimal separable minimax optimization. In *ICML*, 2023.
- T. Lin, C. Jin, and M. I. Jordan. Near-Optimal Algorithms for Minimax Optimization. In *COLT*, 2020.
- E. Z. Liu, B. Haghgoo, A. S. Chen, A. Raghunathan, P. W. Koh, S. Sagawa, P. Liang, and C. Finn. Just Train Twice: Improving Group Robustness without Training Group Information. In *ICML*, 2021.
- J. Liu, Z. Shen, Y. He, X. Zhang, R. Xu, H. Yu, and P. Cui. Towards out-of-distribution generalization: A survey, 2023.
- Z. Liu, Q. Bai, J. Blanchet, P. Dong, W. Xu, Z. Zhou, and Z. Zhou. Distributionally Robust Q -Learning. In *ICML*, 2022.
- K. Lotidis, N. Bambos, J. Blanchet, and J. Li. Wasserstein Distributionally Robust Linear-Quadratic Estimation under Martingale Constraints. In *AISTATS*, 2023.
- R. Mehta, V. Roulet, K. Pillutla, L. Liu, and Z. Harchaoui. Stochastic Optimization for Spectral Risk Measures. In *AISTATS*, 2023.
- R. Mehta, V. Roulet, K. Pillutla, and Z. Harchaoui. Distributionally Robust Optimization with Bias and Variance Reduction. In *ICLR*, 2024.
- H. Namkoong and J. C. Duchi. Stochastic Gradient Methods for Distributionally Robust Optimization with f -divergences. In *NeurIPS*, 2016.
- H. Namkoong and J. C. Duchi. Variance-based Regularization with Convex Objectives. In *NeurIPS*, 2017.
- J. Nocedal and S. J. Wright. *Numerical Optimization*. Springer, 1999.
- B. Palaniappan and F. Bach. Stochastic Variance Reduction Methods for Saddle-Point Problems. *NeurIPS*, 29, 2016.
- R. T. Rockafellar and J. O. Royset. Superquantiles and Their Applications to Risk, Random Variables, and Regression. In *Theory Driven by Influential Applications*. Informs, 2013.
- H. Sapkota, D. Wang, Z. Tao, and Q. Yu. Distributionally Robust Ensemble of Lottery Tickets Towards Calibrated Sparse Network Training. In *NeurIPS*, 2023.
- E. Saravia, H.-C. T. Liu, Y.-H. Huang, J. Wu, and Y.-S. Chen. CARER: Contextualized Affect Representations for Emotion Recognition. In *EMNLP*, 2018.
- V. D. Sharma, M. Toubeh, L. Zhou, and P. Tokekar. Risk-Aware Planning and Assignment for Ground Vehicles using Uncertain Perception from Aerial Vehicles. In *2020 IEEE/RSJ IROS*, 2020.
- C. Song, S. J. Wright, and J. Diakonikolas. Variance reduction via primal-dual accelerated dual averaging for nonsmooth convex finite-sums. In *Proc. ICML'21*, 2021.
- C. Song, C. Y. Lin, S. Wright, and J. Diakonikolas. Coordinate Linear Variance Reduction for Generalized Linear Programming. In *NeurIPS*, 2022.
- A. Tsanas and A. Xifara. Accurate Quantitative Estimation of Energy Performance of Residential Buildings Using Statistical Machine Learning Tools. *Energy and Buildings*, 49, 2012.
- P. Tüfekci. Prediction of Full Load Electrical Power Output of a Base Load Operated Combined Cycle Power Plant using Machine Learning Methods. *International Journal of Electrical Power & Energy Systems*, 60, 2014.
- S. Wang, N. Si, J. Blanchet, and Z. Zhou. A Finite Sample Complexity Bound for Distributionally Robust Q -learning. In *AISTATS*, 2023a.

- Z. Wang, L. Shen, T. Liu, T. Duan, Y. Zhu, D. Zhan, D. Doermann, and M. Gao. Defending against Data-Free Model Extraction by Distributionally Robust Defensive Training. In *NeurIPS*, 2023b.
- O. Wiles, S. Goyal, F. Stimberg, S.-A. Rebuffi, I. Ktena, K. D. Dvijotham, and A. T. Cemgil. A fine-grained analysis on distribution shift. In *ICLR*, 2022.
- G. Xie, L. Luo, Y. Lian, and Z. Zhang. Lower Complexity Bounds for Finite-Sum Convex-Concave Minimax Optimization Problems. In *ICML*, 2020.
- Z. Yang, Y. Guo, P. Xu, A. Liu, and A. Anandkumar. Distributionally Robust Policy Gradient for Offline Contextual Bandits. In *AISTATS*, 2023.
- I. Yeh. Analysis of Strength of Concrete Using Design of Experiments and Neural Networks. *Journal of Materials in Civil Engineering*, 18, 2006.
- Y. Yu, T. Lin, E. V. Mazumdar, and M. Jordan. Fast Distributionally Robust Learning with Variance-Reduced Min-Max Optimization. In *AISTATS*, 2022.
- Z. Yu, L. Dai, S. Xu, S. Gao, and C. P. Ho. Fast Bellman Updates for Wasserstein Distributionally Robust MDPs. In *NeurIPS*, 2023.
- J. Zhang, M. Hong, and S. Zhang. On lower iteration complexity bounds for the convex concave saddle point problems. *Mathematical Programming*, 194, 2022.

Appendix

Appx. A contains all notation introduced throughout the paper. Appx. B discussed convergence rate comparisons in detail with contemporary work. The full convergence analysis of DRAGO is given in Appx. C. A description of the algorithm amenable to implementation is given in Appx. D, whereas experimental settings are described in detail within Appx. E.

Table of Contents

A	Notation	15
B	Comparisons to Existing Literature	16
B.1	Distributionally Robust Optimization (DRO)	16
B.2	Primal-Dual Saddle Point Algorithms	17
C	Convergence Analysis of DRAGO	21
C.1	Overview	21
C.2	Technical Lemmas	23
C.3	Proof of Main Result	29
D	Implementation Details	40
D.1	Algorithm Description	40
D.2	Solving the Maximization Problem	40
E	Experimental Details	44
E.1	Datasets	44
E.2	Hyperparameter Selection	44
E.3	Compute Environment	45
E.4	Additional Experiments	45

A Notation

Symbol	Description
n	Sample size, or number of loss functions.
d	Dimensionality of primal variables.
$\mathcal{W} \subseteq \mathbb{R}^d$	Primal feasible set, which is closed and convex.
$\mathcal{Q} \in \Delta^n$	Ambiguity set, or dual feasible set, which is closed and convex. Here, $\Delta^n = \{p \in [0, 1]^n : \sum_{i=1}^n p_i = 1\}$.
q_0	The uniform vector $q_0 = \mathbf{1}/n = (1/n, \dots, 1/n)$. Used as a dual initialization.
$D(q\ q_0)$	The Bregman divergence between $q \in \mathcal{Q}$ and q_0 , which is 1-strongly convex in its first argument with respect to $\ \cdot\ _2$.
ℓ	Loss function $\ell : \mathcal{W} \rightarrow \mathbb{R}^n$, which is differentiable in each component.
$\mu \geq 0$	Primal regularization constant.
$\nu \geq 0$	Dual regularization constant.
$\mathcal{L}(w, q)$	Objective function $\mathcal{L}(w, q) := q^\top \ell(w) - \nu D(q\ q_0) + \frac{\mu}{2} \ w\ _2^2$.
(w_*, q_*)	Saddle point of \mathcal{L} , which satisfies $\mathcal{L}(w_*, q) \leq \mathcal{L}(w_*, q_*) \leq \mathcal{L}(w, q_*)$ for all $(w, q) \in \mathcal{W} \times \mathcal{Q}$.
$[n]$	Index set $[n] = \{1, \dots, n\}$.
q_{\max}	The value $\max_{q \in \mathcal{Q}} \ q\ _\infty$.
G	Lipschitz continuity constant of each ℓ_i for $i \in [n]$, for which $ \ell_i(w) - \ell_i(w') \leq G \ w - w'\ _2$.
L	Lipschitz continuity constant of each $\nabla \ell_i$ for $i \in [n]$, for which $\ \nabla \ell_i(w) - \nabla \ell_i(w')\ _2 \leq L \ w - w'\ _2$.
$\nabla \ell(w)$	Jacobian matrix of $\ell : \mathbb{R}^d \rightarrow \mathbb{R}^n$ at w (shape = $n \times d$).
(a_t)	Sequence of positive constants that determine the averaging of the gap function.
(A_t)	Sequence of partial sums of (a_t) , or $A_t = \sum_{s=1}^t a_s$. The convergence rate will be given by A_t^{-1} , so we have a_t increase geometrically.
b	Batch or block size.
M	Number of blocks n/b .
(w_t, q_t)	Sequence of primal and dual iterates.
e_j	The j -th standard basis vector $e_j \in \{0, 1\}^n$.
$\hat{\ell}_t$	Loss table, which approximates $\ell(w_t) \in \mathbb{R}^n$.
\hat{g}_t	Gradient table, which approximates $\nabla \ell(w_t) \in \mathbb{R}^{n \times d}$.
\hat{q}_t	Weight table, which approximates $q_t \in \mathcal{Q}$.
$\mathbb{E}_t[\cdot]$	Shorthand for $\mathbb{E}[\cdot \mathcal{H}_{t-1}]$, i.e., expectation conditioned on history $\mathcal{H}_{t-1} = \{(I_s, J_s)\}_{s=1}^{t-1}$.

Table 2: Notation used throughout the paper.

B Comparisons to Existing Literature

In this appendix, we compare our work to existing literature along two axes: 1) distributional robust optimization (DRO), and 2) primal-dual algorithms for saddle-point problems. In the first category, we are primarily concerned with questions of practical and statistical interest, such as which ambiguity sets can be used, how the size of the ambiguity set affects the convergence rate, and what assumptions are needed on the distribution of losses. In the second category, we discuss computational complexity under various assumptions such as smoothness and strong convexity of the objective.

B.1 Distributionally Robust Optimization (DRO)

Examples of DRO Problems Our problem

$$\min_{w \in \mathcal{W}} \max_{q \in \mathcal{Q}} \left[\mathcal{L}(w, q) := q^\top \ell(w) - \nu D(q \| \mathbf{1}/n) + \frac{\mu}{2} \|w\|_2^2 \right] \quad (12)$$

accommodates several settings of interest across machine learning. For example, f -DRO with parameter ρ (Namkoong and Duchi, 2016; Carmon and Hausler, 2022) results by defining the ambiguity set and penalty as

$$\mathcal{Q} = \mathcal{Q}(\rho) := \{q : D_f(q \| \mathbf{1}/n) \leq \rho\} \text{ and } D(q \| \mathbf{1}/n) = D_f(q \| \mathbf{1}/n),$$

where $D_f(q \| p) = \sum_{i=1}^n p_i f(q_i/p_i)$ denotes an f -divergence generated by f (which is always well-defined when $p_i = \mathbf{1}/n$). Common examples include the Kullback-Leibler (KL) divergence, generated by $f_{\text{KL}}(x) = -x \log x$ and the χ^2 -divergence generated by $f_{\chi^2}(x) = (x - 1)^2$. Spectral risk measures (Mehta et al., 2023) are parametrized by an n -length vector $\sigma = (\sigma_1, \dots, \sigma_n)$ such that $0 \leq \sigma_1 \leq \dots \leq \sigma_n$ and $\sum_{i=1}^n \sigma_i = 1$. The penalty in that setting may also be in the form of an f -divergence (Mehta et al., 2024), so that

$$\mathcal{Q} = \mathcal{Q}(\sigma) := \text{conv}(\{\text{permutations of } \sigma\}) \text{ and } D(q \| \mathbf{1}/n) = D_f(q \| \mathbf{1}/n),$$

where $\text{conv}(\cdot)$ denotes the convex hull. The most notable example of such an ambiguity set is the θ -conditional value-at-risk, or CVaR (Rockafellar and Royset, 2013), wherein the largest θn values of σ are set to $1/(n\theta)$ and the remaining are set to zero (with a fractional component if θn is not an integer). Finally, Wasserstein-DRO (Kuhn et al., 2019; Blanchet et al., 2019; Yu et al., 2022) with parameter δ typically sets the ambiguity set to be a δ -ball $\{Q : W_c(Q, P_n) \leq \delta\}$ in Wasserstein distance, where Q is a probability measure, P_n is the empirical measure of the training data, and W_c is the Wasserstein distance associated to cost function c . This differs from f -DRO and spectral risk minimization because in the latter settings, the “shifted” distribution Q is assumed to remain on the same n atoms as before, so that it may simply be specified by a probability vector $q \in [0, 1]^n$ (resp. P_n by $\mathbf{1}/n$). However, as shown by Yu et al. (2022), Wasserstein-DRO can be reformulated into a problem of the form (12) if the following conditions are satisfied: 1) the loss is of a generalized linear model $\ell_i(w) = \Psi(\langle w, x_i \rangle, y_i)$ with feature-label pair (x_i, y_i) and discrepancy function Ψ , 2) the cost function $c((x, y), (x', y'))$ is of the form $\|x - x'\|_2 + \beta |y - y'|$ for $\beta > 0$, and 3) the function Ψ is Lipschitz continuous with known constant.

Directly Using Gradient Descent In the penalized case, we add that the objective $w \mapsto \max_{q \in \mathcal{Q}} \mathcal{L}(w, q)$ is $(L + \mu + \frac{nG^2}{\nu})$ -smooth when the losses ℓ_i are G -Lipschitz continuous and L -smooth. For this reason, we may consider simply applying full-batch gradient descent to this objective, which is included in our comparisons. To see why this smoothness condition holds, define $h(l) := \max_{q \in \mathcal{Q}} \{q^\top l - \nu D(q \| \mathbf{1}/n)\}$, so that when $q \mapsto D(q \| \mathbf{1}/n)$ is 1-strongly convex with respect to $\|\cdot\|_2^2$, it holds that ∇h is $(1/\nu)$ -Lipschitz continuous with respect to $\|\cdot\|_2^2$, and that $\nabla h(l)$ is non-negative and sums to one (i.e. is a probability distribution). Then, by the chain rule, for any $w_1, w_2 \in \mathcal{W}$, we have

that

$$\begin{aligned}
& \left\| \nabla \ell(w_1)^\top \nabla h(\ell(w_1)) - \nabla \ell(w_2)^\top \nabla h(\ell(w_2)) \right\|_2 \\
& \leq \left\| \nabla \ell(w_1)^\top (\nabla h(\ell(w_1)) - \nabla h(\ell(w_2))) \right\|_2 + \left\| (\nabla \ell(w_1) - \nabla \ell(w_2))^\top \nabla h(\ell(w_2)) \right\|_2 \\
& \leq \frac{nG}{\nu} \|\ell(w_1) - \ell(w_2)\|_2 + L \|w_1 - w_2\|_2^2 \\
& \leq \left(\frac{nG^2}{\nu} + L \right) \|w_1 - w_2\|_2^2.
\end{aligned}$$

Thus, when referring to the gradient descent on $w \mapsto \max_{q \in \mathcal{Q}} \mathcal{L}(w, q) = h(\ell(w)) + \frac{\mu}{2} \|w\|_2^2$, we reference the smoothness constant $\left(L + \mu + \frac{nG^2}{\nu} \right)$.

Comparison of DRO Approaches The performance of classical and recent algorithms designed for the problems above is detailed in Tab. 3. The rightmost column displays the **oracle complexity**, meaning the number of queries to individual/component loss functions $\{(\ell_i, \nabla \ell_i)\}$ as a function of the desired suboptimality ε . The desiderata in the large-scale setting is to decouple the contribution of the sample size n and the condition number in smooth, strongly convex settings ($\mu > 0$ and $L < \infty$) or the quantity $1/\varepsilon$ in non-smooth or non-strongly convex settings. For readability, we encode **dependence on n** in red and **dependence on $1/\varepsilon$** in blue within Tab. 3. In certain cases, such as in the sub-gradient method, the dependence on n is understood as part of a smoothness constant. Similarly, because q_{\max} is of order $1/n$ in the best case and 1 in the worst case, we interpret nq_{\max} to play the role of a condition number that measures the size of the ambiguity set. These instances of n are left uncolored.

The closest comparison to our setting is that of LSVRG (Mehta et al., 2023) and Prospect (Mehta et al., 2024). Including DRAGO, these methods all achieve linear convergence on (12), under the assumption of strongly convex regularization in the primal objective. However, both LSVRG and Prospect demand a stringent lower bound of $\Omega(nG^2/\mu)$ on the dual regularization parameter ν to achieve this rate, which essentially matches ours in this regime (as $\sqrt{nG^2}/(\mu\nu)$ reduces to a constant). When this condition does not hold, however, LSVRG does not have a convergence guarantee while Prospect underperforms against the sub-gradient method. DRAGO, on the other hand, is the only method that achieves unconditional linear convergence and fully captures the dependence on the dual regularization parameter ν , which is a smoothness measure of the objective $\max_q \mathcal{L}(w, q)$.

Moving to methods that are not linearly convergent, Levy et al. (2020) consider a variant of mini-batch SGD that solves the maximization problem within the mini-batch itself. In Tab. 3, we include a term $\min\{n, b(\varepsilon)\}$. This is because Levy et al. (2020) considers the fully stochastic setting, in which samples from the underlying data-generating distribution are generated on each iterate. Thus, the convergence bounds are achieved by choosing a batch size $b(\varepsilon)$ large enough to reduce finite-sample bias between a surrogate objective and the true distributionally robust objective, whereas the remaining term is an optimization error on the surrogate. Thus, in the incremental setting (in which there is a fixed training set of size n) we add the minimum to account for the case in which the theoretically required batch size grows so large that it exceeds the full batch size itself. Indeed, as commented by Carmon and Hausler (2022), when the ambiguity set is large (i.e. θ is small for CVaR and ρ is large for χ^2 -divergence), the method may underperform against the sub-gradient method. This is true of methods such as Mehta et al. (2024) and ours that depend on $nq_{\max} \leq n$. This indicates that across DRO settings, increased ambiguity set sizes can bring the performance of incremental methods arbitrarily close to that of the full-batch sub-gradient method. Finally, notice that DRAGO also has a dependence on the batch size b in Tab. 3. While it would appear that $b = 1$ would minimize oracle complexity, we describe in the next section how b can be chosen to minimize global complexity, which includes the cost of each oracle call as a function of the primal dimension d . Because of the diversity of settings, a coarser measure such as first-order oracle evaluations may be sufficient to compare methods along the DRO axis; we use finer-grained complexity measures to compare methods along the axis of saddle-point algorithms.

B.2 Primal-Dual Saddle Point Algorithms

In order to make comparisons among methods for general min-max problems, we first identify aspects of (12) that make it a highly specialized problem in this regard. The major points include:

1. The objective has a *finite-sum* structure, in that it can be written as $\sum_{i=1}^n f_i(w, q)$, where $f_i(w, q) := q_i \ell_i(w) -$

$$\nu D(q|\mathbf{1}/n) + \frac{\mu}{2} \|w\|_2^2.$$

2. The dimension of the dual variable q is equal to n , the number of functions in the sum (i.e. the sample size).
3. The dual regularizer $q \mapsto D(q|\mathbf{1}/n)$ is not necessarily smooth. This encompasses common statistical divergences such as the Kullback Leibler (KL).

For discussions in which linear convergence is a pre-requisite, it is typically assumed that $(w, q) \mapsto \mathcal{L}(w, q)$ is a smooth map, and finer-grained results depend on the individual Lipschitz continuity parameters of $w \mapsto \nabla_w \mathcal{L}(w, q)$, $q \mapsto \nabla_q \mathcal{L}(w, q)$, $w \mapsto \nabla_w \ell(w)$, and $q \mapsto \nabla_w \mathcal{L}(w, q)$. Second, noting that the dual variable dimension is n , it would be non-trivial to achieve a global complexity that is not quadratic in n . To make the regularized DRO setting of (12) comparable to classical and contemporary saddle-point methods, we make the additional assumption in this section that the (rescaled) χ^2 -divergence penalty is used, so that $D(q|\mathbf{1}/n) = \frac{1}{2} \|q - \mathbf{1}/n\|_2^2$ and we may compute the [smoothness constants](#) as

$$\|\nabla_w \mathcal{L}(w, q) - \nabla_w \mathcal{L}(w', q)\|_2 \leq (L + \mu) \|w - w'\|_2$$

$$\|\nabla_w \mathcal{L}(w, q) - \nabla_w \mathcal{L}(w, q')\|_2 = \|\nabla \ell(w)^\top (q - q')\|_2 \leq \sqrt{n}G \|q - q'\|_2$$

$$\|\nabla_q \mathcal{L}(w, q) - \nabla_q \mathcal{L}(w, q')\|_2 \leq \nu \|q - q'\|_2 \tag{13}$$

$$\|\nabla_q \mathcal{L}(w, q) - \nabla_q \mathcal{L}(w', q)\|_2 = \|\ell(w) - \ell(w')\|_2 \leq \sqrt{n}G \|w - w'\|_2 \tag{14}$$

$$\|\nabla_{(w,q)} \mathcal{L}(w, q) - \nabla_{(w,q)} \mathcal{L}(w', q')\|_2 \leq (\max\{L + \mu, \nu\} + \sqrt{n}G) \sqrt{2} \|(w, q) - (w', q')\|_2. \tag{15}$$

In making this assumption, however, we emphasize that our results *do not depend on* (13), (14), and (15) being true. We assume here that calls to the oracles $(\ell_i, \nabla_w \ell_i)$ cost $O(d)$ operations while calls to $\nabla_q \mathcal{L}$ cost $O(n)$ operations, making the total $O(n + d)$. This per-iteration complexity is a subtlety of DRO which is essential to recognize when comparing methods. With DRAGO, we also have a batch size parameter b , setting the complexity to $O(n + bd)$. By tuning b , we may achieve improvements in terms of global complexity over standard primal-dual methods. Results comparing linearly convergent methods in terms of the global complexity of elementary operations are given in Tab. 4. The table contains a ‘‘half-life’’ column, which is the constant τ multiplied with $\log(1/\varepsilon)$ when describing the number of iterations needed to reach ε -suboptimality as $\tau \log(1/\varepsilon)$. Before comparisons, observe that the optimal batch size for DRAGO is $b = n/d$, in the sense that the global number of arithmetic operations is of order

$$n \frac{Lnq_{\max}}{\mu} + nd \sqrt{\frac{nG^2}{\mu\nu}}$$

This is an improvement over setting $b = 1$, in which case the same number is

$$(n + d) \frac{Lnq_{\max}}{\mu} + n(n + d) \sqrt{\frac{nG^2}{\mu\nu}}$$

Next, the most comparable and recent setting is that of [Li et al. \(2023\)](#). Notice that DRAGO is able to improve by a factor of d on the $\frac{L}{\mu}$ term, as long as $nq_{\max} = O(1)$. The number nq_{\max} can typically be bounded above by a quantity independent of n (for example, the bound is $1/\theta$ for the θ -CVaR ([Mehta et al., 2023](#))).

While less comparable, we mention known lower bounds for completeness. In terms of lower bounds, since (12) enjoys a particular structure, such as decomposability into so-called *marginal* terms $\nu D(q|\mathbf{1}/n)$ and $\frac{\mu}{2} \|w\|_2^2$ and a *coupled* term $q^\top \ell(w)$, we are not necessarily constrained by the more general lower bounds of [Zhang et al. \(2022\)](#) and [Xie et al. \(2020\)](#). For example, the proximal incremental first-order (PIFO) model of [Xie et al. \(2020\)](#) assumes that we observe first-order information from a single component in the sum; in DRAGO, using a batch size of n/d is required to achieve the desired improvement. [Zhang et al. \(2022\)](#), on the other hand, do not treat the finite sum class of problems considered here. Furthermore, we still list the per-iteration cost as $O(n + d)$ because a single PIFO call to the dual gradient is of size n .

Method	Assumptions	Ambiguity Set	Evaluations of $\{(\ell_i, \nabla \ell_i)\}_{i=1}^n$ Components (Big- \tilde{O})
Sub-Gradient Method	ℓ_i is G -Lipschitz $\ w - w'\ _2 \leq R$ (if included) $\mu > 0$ (if included) $\nabla \ell_i$ is L -Lipschitz and $\nu > 0$ (if included)	Any Any Any	$n \cdot (GR)^2 \varepsilon^{-2}$ $n \cdot G^2 \mu^{-1} \varepsilon^{-1}$ $n \cdot \mu^{-1} (L + \mu + nG^2/\nu) \log(1/\varepsilon)$
$\mathcal{L}_{\text{CVaR-SGD}}$	ℓ_i is G -Lipschitz and in $[0, B]$	θ -CVaR †	$\min\{n, B^2 \theta^{-1} \varepsilon^{-2}\} \cdot (GR)^2 \varepsilon^{-2}$
$\mathcal{L}_{\chi^2\text{-SGD}}$	ℓ_i is G -Lipschitz and in $[0, B]$	ρ -ball in χ^2 -divergence §	$\min\{n, (1 + \rho)B^2 \varepsilon^{-2}\} \cdot (GR)^2 \varepsilon^{-2}$
$\mathcal{L}_{\chi^2\text{-pen-SGD}}$ (Levy et al., 2020)	$\ w - w'\ _2 \leq R$ for all $w, w' \in \mathbb{W}$ $\nu > 0$ (if included)	χ^2 -divergence penalty §	$\min\{n, B^2 \nu^{-1} \varepsilon^{-1}\} \cdot (GR)^2 \varepsilon^{-2}$
BROO*	ℓ_i is G -Lipschitz	1-ball in f -divergence	$n \cdot (GR)^{2/3} \varepsilon^{-2/3} + (GR)^2 \varepsilon^{-2}$
BROO*	$\ w - w'\ _2 \leq R$ for all $w, w' \in \mathbb{W}$	1-ball in f -divergence	$n \cdot (GR)^{2/3} \varepsilon^{-2/3} + n^{3/4} (GR \varepsilon^{-1} + L^{1/2} R \varepsilon^{-1/2})$
(Carmon and Hausler, 2022)	$\nabla \ell_i$ is L -Lipschitz (if included)		
SEVR	$\nabla \ell_i$ is L -Lipschitz	Wasserstein-DRO in GLMs	$n \log(1/\varepsilon) + D_{\text{loss}} \varepsilon^{-1} + L^2 D_w^4 \varepsilon^{-2}$
SPPRR	$\ w_0 - w_*\ _2 \leq D_w$	Wasserstein-DRO in GLMs	$(L^2 D_w^2 \varepsilon^{-1} + D_w^2 \varepsilon^{-2}) \log(1/\varepsilon)$
(Yu et al., 2022)	$\max_q \mathcal{L}(w_0, q) - \mathcal{L}(w_*, q_*) \leq D_{\text{loss}}$		
LSVRG	ℓ_i is G -Lipschitz	Spectral Risk Measures (ν small)	None
LSVRG	$\nabla \ell_i$ is L -Lipschitz	Spectral Risk Measures ($\nu \geq \Omega(nG^2/\mu)$)	$(n + nq_{\max} \kappa) \log(1/\varepsilon)$
(Mehta et al., 2023)	$\mu > 0, \nu > 0, \kappa := (L + \mu)/\mu$		
Prospect	ℓ_i is G -Lipschitz	Spectral Risk Measures (ν small)	$n (nq_{\max} \kappa + G^4/(\mu^2 \nu^2) \max\{\kappa^2, G^2/(\mu \nu)\}) \log(1/\varepsilon)$
Prospect	$\nabla \ell_i$ is L -Lipschitz	Spectral Risk Measures ($\nu \geq \Omega(nG^2/\mu)$)	$(n + nq_{\max} \kappa) \log(1/\varepsilon)$
(Mehta et al., 2024)	$\mu > 0, \nu > 0, \kappa := (L + \mu)/\mu$		
DRAGO (Ours)	ℓ_i is G -Lipschitz $\nabla \ell_i$ is L -Lipschitz $\mu > 0, \nu > 0, b := \text{Batch Size}$	Any	$(n + bnq_{\max} L/\mu + n\sqrt{nG^2/(\mu \nu)}) \log(1/\varepsilon)$

Table 3: Replicate of Tab. 1.

Method	Assumptions	Half-Life	Per-Iteration Cost
Sub-Gradient Method		$\frac{L+\mu}{\mu} + \frac{nG^2}{\mu\nu}$	nd
Minimax-APPA (Lin et al., 2020)		$\frac{(L+\mu)\vee\nu+\sqrt{n}G}{\sqrt{\mu\nu}}$	nd
Lower Bound (Xie et al., 2020)	Finite Sum Single component oracle May not be decomposable	$n + \frac{(L+\mu)\vee\nu+\sqrt{n}G}{\min\{\mu,\nu\}}$	$n + d$
Lower Bound (Zhang et al., 2022)	May not be decomposable May not be finite sum	$\sqrt{\frac{L+\mu}{\mu} + \frac{nG^2}{\mu\nu}}$	nd
AG-OG with Restarts (Li et al., 2023)		$\frac{L}{\mu} \vee \sqrt{\frac{nG^2}{\mu\nu}}$	nd
Drago ($b = 1$)	$D(\cdot\ \mathbf{1}/n)$ need not be smooth	$\frac{Lnq_{\max}}{\mu} + n\sqrt{\frac{nG^2}{\mu\nu}}$	$n + d$
Drago ($b = n/d$)		$\frac{Lnq_{\max}}{\mu} + d\sqrt{\frac{nG^2}{\mu\nu}}$	n
Drago ($b = n$)		$\frac{Lnq_{\max}}{\mu} + \sqrt{\frac{nG^2}{\mu\nu}}$	nd

Table 4: **Complexity of Primal-Dual Saddle Point Methods.** Half-life (defined as τ such that a linearly convergent method requires $O(\tau \log(1/\varepsilon))$ iterations to achieve ε -suboptimality) and per-iteration cost of linearly convergent optimization algorithms. The global number of arithmetic operations (under the assumption that $(\ell_i, \nabla_w \ell_i)$ costs $O(d)$ operations and $\nabla_q \mathcal{L}$ costs $O(n)$ operations) required to achieve a point (w, q) satisfying $\mathcal{L}(w, q_*) - \mathcal{L}(w_*, q) \leq \varepsilon$ can be computed by multiplying the last two columns. The ‘‘Assumptions’’ column contains changes to the assumptions that each ℓ_i is L -smooth and that $D(\cdot\|\mathbf{1}/n)$ is ν -smooth.

C Convergence Analysis of DRAGO

This section provides the convergence analysis for DRAGO. We first recall the quantities of interest and provide an alternate description of the algorithm that is useful for understanding the analysis. A high-level overview is given in Appx. C.1, and the remaining subsections comprise steps of the proof.

C.1 Overview

See Tab. 2 for a reference on notation used throughout the proof, which will also be introduced as it appears. Define $q_0 = \mathbf{1}/n$ and recall the objective

$$\mathcal{L}(w, q) := q^\top \ell(w) - \nu D(q \| q_0) + \frac{\mu}{2} \|w\|_2^2. \quad (16)$$

By strong convexity of $w \mapsto \max_q \mathcal{L}(w, q)$ with respect to $\|\cdot\|_2$ and strong concavity of $q \mapsto \min_w \mathcal{L}(w, q)$ with respect to $\|\cdot\|_2$, a primal-dual solution pair (w^*, q^*) is guaranteed to exist and is unique, and thus we define

$$w_\star = \arg \min_{w \in \mathcal{W}} \max_{q \in \mathcal{Q}} \mathcal{L}(w, q) \text{ and } q_\star = \arg \max_{q \in \mathcal{Q}} \min_{w \in \mathcal{W}} \mathcal{L}(w, q).$$

We describe the algorithm, the optimality criterion, and the proof outline.

Algorithm Description First, we describe two sequences of parameters that are used to weigh various terms in the primal and dual updates. The parameters are set in the analysis, and the version of the algorithm in Sec. 3 is a description with these values plugged in. However, we keep them as variables in this section to better describe the logic of the proof.

Specifically, let $(a_t)_{t \geq 1}$ be a sequence of positive numbers and define $a_0 = 0$ in addition. Denote $A_t = \sum_{s=1}^T a_s$. These will become the averaging sequence that will aggregate successive gaps γ_t (see (23)) into the return value $\sum_{t=1}^T a_t \gamma_t$, which will be upper bounded by a constant in T (in expectation). We also define another similar sequence $(c_t)_{t \geq 1}$, and define $C_t = A_t - (n/b - 1)c_t$ for batch size b . We assume for simplicity that b divides n . When all constants are set, the algorithm will reduce to that given in Algorithm 1. We have one hyperparameter $\eta > 0$, which may be interpreted as a learning rate.

Using initial values $w_0 = 0$ and $q_0 = \mathbf{1}/n$, initialize the tables $\hat{\ell}_0 = \ell(w_0) \in \mathbb{R}^n$, $g_0 = \nabla \ell(w_0) \in \mathbb{R}^{n \times d}$, and $\hat{q}_0 = q_0 \in \mathbb{R}^n$. In addition, partition the $[n]$ sample indices into $M := n/b$ blocks of size b , or B_1, \dots, B_M with $B_K := ((K-1)b+1, \dots, Kb)$ for $K \in [M]$. We can set the averaging sequence according to the following scheme:

$$a_1 = 1, a_2 = 4\eta, \text{ and } a_t = (1 + \eta) a_{t-1} \text{ for } t > 2.$$

The initial value $a_2 = 4\eta$ is a slight modification for theoretical convenience, and the algorithm operates exactly as in Sec. 3 in practice. In order to retrieve the Sec. 3 version, we simply replace the condition above with $a_t = (1 + \eta) a_{t-1}$ for $t \geq 2$.

Consider iterate $t \in \{1, \dots, T\}$. We sample a random block I_t uniformly from $[M]$ and compute the primal update.

$$\delta_t^P := \frac{1}{b} \sum_{i \in B_{I_t}} (q_{t-1, i} \nabla \ell_i(w_{t-1}) - \hat{q}_{t-2, i} \hat{g}_{t-2, i}) \quad (17)$$

$$v_t^P := \hat{g}_{t-1}^\top \hat{q}_{t-1} + \frac{na_{t-1}}{a_t} \delta_t^P \quad (18)$$

$$w_t := \arg \min_{w \in \mathcal{W}} a_t \langle v_t^P, w \rangle + \frac{a_t \mu}{2} \|w\|_2^2 + \frac{C_{t-1} \mu}{2} \|w - w_{t-1}\|_2^2 + \frac{c_{t-1} \mu}{2} \sum_{s=t-n/b}^{t-2} \|w - w_{s \vee 0}\|_2^2 \quad (19)$$

We see that $C_{t-1} + c_{t-1}(n/b - 1) = A_{t-1}$, so the inner objective of the proximal operator (19) is $A_t \mu$ -strongly convex (as the one in (22) is $A_t \nu$ -strongly concave). Note that when $n/b < 1$, we simply treat the method as not including the additional regularization term $\frac{c_{t-1} \mu}{2} \sum_{s=t-n/b}^{t-2} \|w - w_{s \vee 0}\|_2^2$. Proceeding, we then modify the loss and gradient

table. The loss update has to occur between the primal and dual updates to achieve control over the variation in the dual update (see Appx. C.2). Define $K_t = t \bmod M + 1$ as the (deterministic) block to be updated, and set

$$(\hat{\ell}_{t,k}, \hat{g}_{t,k}) = \begin{cases} (\ell_k(w_t), \nabla \ell_k(w_t)) & \text{if } k \in B_{K_t} \\ (\hat{\ell}_{t-1,k}, \hat{g}_{t-1,k}) & \text{otherwise} \end{cases}.$$

Define e_j to be the j -th standard basis vector. Then, sample a random block J_t uniformly from $[M]$ compute

$$\delta_t^D := \frac{1}{b} \sum_{j \in B_{J_t}} (\ell_j(w_t) - \hat{\ell}_{t-1,j}) e_j \quad (20)$$

$$v_t^D := \hat{\ell}_t + \frac{na_{t-1}}{a_t} \delta_t^D \quad (21)$$

$$q_t := \arg \max_{q \in \mathcal{Q}} a_t \langle v_t^D, q \rangle - a_t \nu D(q \| q_0) - A_{t-1} \nu \Delta_D(q, q_{t-1}). \quad (22)$$

Notice the change in indices between (17) and (21), which accounts for the update in the loss table that occurs in between. Finally, we must update the remaining table. Set

$$\hat{q}_{t,k} = \begin{cases} q_{t,k} & \text{if } k \in B_{K_t} \\ \hat{q}_{t-1,k} & \text{otherwise} \end{cases}.$$

We define the random variable $\mathcal{H}_t := \{(I_s, J_s)\}_{s=1}^t$ as the history of blocks selected at all times up to and including t , and define $\mathbb{E}_t[\cdot]$ to be the conditional expectation operator given \mathcal{H}_{t-1} . In other words, \mathbb{E}_t integrates the randomness $\{(I_s, J_s)\}_{s=t}^T$. Accordingly $\mathbb{E}_1[\cdot]$ is the marginal expectation of the entire random process. We may now describe the optimality criterion.

Proof Outline Construct the gap function

$$\gamma_t = a_t \left(\mathcal{L}(w_t, q_\star) - \mathcal{L}(w_\star, q_t) - \frac{\mu}{2} \|w_t - w_\star\|_2^2 - \frac{\nu}{2} \|q_t - q_\star\|_2^2 \right) \quad (23)$$

and aim to bound $\mathbb{E}_1 \left[\sum_{s=1}^t \gamma_s \right]$ by a constant. Throughout the proof, we will use a free parameter α , which relates to η according to the relation

$$a_t \leq (1 + \eta) a_{t-1} \implies a_t \leq \min \left\{ \left(1 + \frac{\alpha}{4}\right) a_{t-1}, \alpha A_{t-1}, 4\alpha(n/b - 1)^2 C_{t-1} \right\}. \quad (24)$$

For readability, we assume the right-hand side of (24) holds in **Step 1** and **Step 2**. We then select η to satisfy this condition (and all others) in **Step 3** below. The proof occurs in five steps total.

1. Lower bound the dual suboptimality $a_t \mathcal{L}(w_\star, q_t)$.
2. Upper bound the primal suboptimality $a_t \mathcal{L}(w_t, q_\star)$, and combine both to derive a bound on the gap function for $t \geq 2$.
3. Derive all conditions on the learning rate constant η and batch size b .
4. Bound γ_1 and sum γ_t over t for a T -step progress bound.
5. Bound the remaining non-telescoping terms to complete the analysis.

We begin with a section of technical lemmas that will not only be useful in various areas of the proof but also capture the main insights that allow the method to achieve the given rate. Given these lemmas, the main proof occurs in Appx. C.3 and otherwise follows standard structure.

C.2 Technical Lemmas

This section contains a number of lemmas that describe common structures in the analysis of quantities in the primal and dual. Lem. 2 bounds cross terms that arise when there are inner products between the primal-dual iterates and their gradient estimates. Lem. 3 and Lem. 4 are respectively the primal and dual noise bounds, constructed to control the variation of the terms δ_t^P and δ_t^D appearing in (17). Finally, Lem. 8 exploits the cyclic style updates of the \hat{q}_t table to bound the term $\|\hat{q}_{t-1} - q_{t-2}\|_2^2$ which is used in the primal noise bound.

Cross Term Bound Both of the estimates of the gradient of the coupled term $q^\top \ell(w)$ with respect to the primal and dual variables share a similar structure (see (18) and compare to (25)). They are designed to achieve a particular form of telescoping, with a remaining squared term that can be controlled by case-specific techniques. This can be observed within Lem. 2. In the sequel, we will refer to a sequence of random vectors $(u_t)_{t \geq 1}$ as *adapted to \mathcal{H}_t* , where $\mathcal{H}_t = \{(I_s, J_s)\}_{s=1}^t$ is the history of random blocks. This simply means that u_t , when conditioned on \mathcal{H}_{t-1} , is only a function of the current random block (I_t, J_t) . Similarly, conditioned on \mathcal{H}_{t-1} , we have that u_{t-1} is not random. In the language of probability theory, $\{\sigma(\mathcal{H}_t)\}_{t \geq 1}$ forms a filtration and u_t is $\sigma(\mathcal{H}_t)$ -measurable, but this terminology is not necessary for understanding the results.

Lemma 2 (Cross Term Bound). *Let $(x_t)_{t \geq 1}$, $(y_t)_{t \geq 1}$, and $(\hat{y}_t)_{t \geq 1}$ denote random sequences of \mathbb{R}^m -valued vectors, and let $x_\star \in \mathbb{R}^m$ be a vector. Denote by I_t be the index of a uniform random block $[M]$.*

$$v_t := \hat{y}_{t-1} + \frac{na_{t-1}}{a_t} \frac{1}{b} \sum_{i \in B_{I_t}} (y_{t-1,i} - \hat{y}_{t-2,i}) \quad (25)$$

Finally, let $(x_t, y_t, \hat{y}_t)_{t \geq 1}$ adapted to \mathcal{H}_t (as defined above). Then, for any positive constant $\gamma > 0$,

$$\begin{aligned} a_t \mathbb{E}_t [\langle y_t - v_t, x_\star - x_t \rangle] &\leq a_t \mathbb{E}_t [\langle y_t - \hat{y}_{t-1}, x_\star - x_t \rangle] - a_{t-1} \langle y_{t-1} - \hat{y}_{t-2}, x_\star - x_{t-1} \rangle \\ &\quad + \frac{n^2 a_{t-1}^2}{2\gamma} \mathbb{E}_t \left\| \frac{1}{b} \sum_{i \in B_{I_t}} (y_{t-1,i} - \hat{y}_{t-2,i}) \right\|_2^2 + \frac{\gamma}{2} \mathbb{E}_t \|x_t - x_{t-1}\|_2^2. \end{aligned}$$

Proof. By plugging in the value of v_t and using $x_\star - x_t = x_\star - x_{t-1} + x_{t-1} - x_t$, we have that

$$\begin{aligned} a_t \mathbb{E}_t [\langle y_t - v_t, x_\star - x_t \rangle] &= a_t \mathbb{E}_t [\langle y_t - \hat{y}_{t-1}, x_\star - x_t \rangle] - na_{t-1} \mathbb{E}_t \left[\left\langle \frac{1}{b} \sum_{i \in B_{I_t}} (y_{t-1} - \hat{y}_{t-2}), x_\star - x_t \right\rangle \right] \\ &= a_t \mathbb{E}_t [\langle y_t - \hat{y}_{t-1}, x_\star - x_t \rangle] - a_{t-1} \langle y_{t-1} - \hat{y}_{t-2}, x_\star - x_{t-1} \rangle \\ &\quad + na_{t-1} \mathbb{E}_t \left[\left\langle \frac{1}{b} \sum_{i \in B_{I_t}} (y_{t-1} - \hat{y}_{t-2}), x_t - x_{t-1} \right\rangle \right] \\ &\leq a_t \mathbb{E}_t [\langle y_t - \hat{y}_{t-1}, x_\star - x_t \rangle] - a_{t-1} \langle y_{t-1} - \hat{y}_{t-2}, x_\star - x_{t-1} \rangle \\ &\quad + \frac{n^2 a_{t-1}^2}{2\gamma} \mathbb{E}_t \left\| \frac{1}{b} \sum_{i \in B_{I_t}} (y_{t-1,i} - \hat{y}_{t-2,i}) \right\|_2^2 + \frac{\gamma}{2} \mathbb{E}_t \|x_t - x_{t-1}\|_2^2, \end{aligned}$$

where the final step follows from Young's inequality with parameter γ . \square

In the primal case, we have that $v_t = v_t^P$, $y_t = \nabla \ell(w_t)^\top q_t$, $\hat{y}_t = \hat{y}_t^\top \hat{q}_t$, and $x_t = w_t$. In the dual case, we have that $v_t = v_t^D$, $y_t = \ell(w_t)$, $\hat{y}_t = \hat{\ell}_{t+1}$, and $x_t = q_t$. The next few lemmas control the third term appearing in Lem. 2 for the specific case of the primal and dual sequences.

Noise Term Bounds Next, we proceed to control the δ_t^P and δ_t^D by way of Lem. 3 and Lem. 4. As discussed in Sec. 2, a key step in the convergence proof is establishing control over these terms. Define $\pi(t, i)$ to satisfy $\hat{q}_{t,i} = q_{\pi(t,i),i}$ and $g_{t,i} = \nabla \ell_i(w_{\pi(t,i)})$, that is, the time index of the last update of table element i on or before time t . This notation is used to write the table values such as \hat{q}_t in terms of past values of the iterates (e.g., q_t).

Lemma 3 (Primal Noise Bound). *When $t \geq 2$, we have that*

$$\begin{aligned}
\mathbb{E}_t \|\delta_t^{\text{P}}\|_2^2 &\leq \frac{3q_{\max}}{n} \sum_{i=1}^n q_{t-1,i} \|\nabla \ell_i(w_{t-1}) - \nabla \ell_i(w^*)\|_2^2 \\
&\quad + \frac{3q_{\max}}{n} \sum_{i=1}^n q_{\pi(t-2,i),i} \|\nabla \ell_i(w_{\pi(t-2,i)}) - \nabla \ell_i(w^*)\|_2^2 \\
&\quad + \frac{3G^2}{n} \|q_{t-1} - \hat{q}_{t-2}\|_2^2
\end{aligned} \tag{26}$$

Proof. By definition, we have that

$$\begin{aligned}
\mathbb{E}_t \|\delta_t^{\text{P}}\|_2^2 &= \mathbb{E}_t \left[\left\| \frac{1}{b} \sum_{i \in B_{I_t}} \nabla \ell_i(w_{t-1}) q_{t-1,i} - \hat{g}_{t-2,i} \hat{q}_{t-2,i} \right\|_2^2 \right] \\
&= \frac{1}{b^2} \mathbb{E}_t \left[\left\| \sum_{i \in B_{I_t}} \nabla \ell_i(w_{t-1}) q_{t-1,i} - \hat{g}_{t-2,i} \hat{q}_{t-2,i} \right\|_2^2 \right] \\
&\leq \frac{1}{b} \mathbb{E}_t \left[\left\| \sum_{i \in B_{I_t}} \nabla \ell_i(w_{t-1}) q_{t-1,i} - \hat{g}_{t-2,i} \hat{q}_{t-2,i} \right\|_2^2 \right] \\
&= \frac{1}{n} \sum_{i=1}^n \|\nabla \ell_i(w_{t-1}) q_{t-1,i} - \hat{g}_{t-2,i} \hat{q}_{t-2,i}\|_2^2,
\end{aligned}$$

where we use that I_t is drawn uniformly over n/b . Continuing again with the term above, we have

$$\begin{aligned}
&\frac{1}{n} \sum_{i=1}^n \|\nabla \ell_i(w_{t-1}) q_{t-1,i} - \hat{g}_{t-2,i} \hat{q}_{t-2,i}\|_2^2 \\
&= \frac{1}{n} \sum_{i=1}^n \|(\nabla \ell_i(w_{t-1}) - \nabla \ell_i(w_\star)) q_{t-1,i} - (\hat{g}_{t-2,i} - \nabla \ell_i(w_\star)) \hat{q}_{t-2,i} + (q_{t-1,i} - \hat{q}_{t-2,i}) \nabla \ell_i(w_\star)\|_2^2 \\
&\leq \frac{3}{n} \sum_{i=1}^n \left(q_{t-1,i}^2 \|\nabla \ell_i(w_{t-1}) - \nabla \ell_i(w_\star)\|_2^2 + \hat{q}_{t-2,i}^2 \|\hat{g}_{t-2,i} - \nabla \ell_i(w_\star)\|_2^2 \right. \\
&\quad \left. + (q_{t-1,i} - \hat{q}_{t-2,i})^2 \|\nabla \ell_i(w_\star)\|_2^2 \right) \\
&\leq \frac{3}{n} \sum_{i=1}^n \left(q_{\max} q_{t-1,i} \|\nabla \ell_i(w_{t-1}) - \nabla \ell_i(w_\star)\|_2^2 + q_{\max} \hat{q}_{t-2,i} \|\hat{g}_{t-2,i} - \nabla \ell_i(w_\star)\|_2^2 \right. \\
&\quad \left. + (q_{t-1,i} - \hat{q}_{t-2,i})^2 G^2 \right).
\end{aligned}$$

where we use that $\|\nabla \ell_i(w_\star)\|_2^2 \leq G^2$ because every ℓ_i is G -Lipschitz with respect to $\|\cdot\|_2^2$, and that $q_i \leq q_{\max} = \max_{q \in \mathcal{Q}} \|q\|_\infty$. This completes the proof. \square

The corresponding dual noise bound in Lem. 4 follows similarly, using coordinate-wise updates.

Lemma 4 (Dual Noise Bound). *For $t \geq 2$,*

$$\mathbb{E}_t \|\delta_t^{\text{D}}\|_2^2 \leq \frac{G^2}{n} \sum_{\tau=t-n/b}^{t-2} \|w_{t-1} - w_{\tau \vee 0}\|_2^2.$$

Proof. Then, we may exploit the coordinate structure of the noise term to write

$$\begin{aligned}
\mathbb{E}_t \|\delta_t^D\|_2^2 &= \mathbb{E}_t \left\| \frac{1}{b} \sum_{j \in B_{J_t}} (\ell_j(w_{t-1}) - \hat{\ell}_{t-1,j}) e_j \right\|_2^2 \\
&= \frac{1}{b^2} \left(\mathbb{E}_t \sum_{j \in B_{J_t}} \left\| (\ell_j(w_{t-1}) - \hat{\ell}_{t-1,j}) e_j \right\|_2^2 \right. \\
&\quad \left. + \mathbb{E}_t \left[\sum_{j \neq k} (\ell_j(w_{t-1}) - \hat{\ell}_{t-1,j}) (\ell_k(w_{t-1}) - \hat{\ell}_{t-1,k}) \langle e_j, e_k \rangle \right] \right) \\
&= \frac{1}{b^2} \mathbb{E}_t \sum_{j \in B_{J_t}} \left\| (\ell_j(w_{t-1}) - \hat{\ell}_{t-1,j}) e_j \right\|_2^2 \\
&= \frac{1}{b^2} \mathbb{E}_t \sum_{j \in B_{J_t}} [|\ell_j(w_{t-1}) - \hat{\ell}_{t-1,j}|^2] \\
&\leq \frac{1}{bn} \sum_{i=1}^n |\ell_i(w_{t-1}) - \hat{\ell}_{t-1,i}|^2 \\
&\leq \frac{G^2}{n} \sum_{\tau=t-n/b}^{t-2} \|w_{t-1} - w_{\tau \vee 0}\|_2^2.
\end{aligned}$$

The red term is zero because $j \neq k$. The sum in the last line has $n/b - 1$ terms because our order of updates forces one of the blocks of the $\hat{\ell}_{t-1}$ vector to have values equal to w_{t-1} before defining δ_t^D . \square

Controlling the Recency of the Loss Table In this section, we bound the $\|q_{t-1} - \hat{q}_{t-2}\|_2^2$ term appearing in the primal noise bound Lem. 3. Controlling this term is essential to achieving the correct rate, as we comment toward the end of this section. The proofs in this section are long but require relatively simple computations.

Recall that the $[n]$ indices are partitioned into blocks (B_1, \dots, B_M) for $M := n/b$, where b is assumed to divide n . For any $t \geq 1$, we first decompose

$$\sum_{i=1}^n (q_{t,i} - \hat{q}_{t-1,i})^2 = \sum_{K=1}^M \sum_{i \in B_K} (q_{t,i} - \hat{q}_{t-1,i})^2,$$

and analyze block-by-block. Our goal is to be able to count this quantity in terms of $\|q_t - q_{t-1}\|_2^2$ terms. The main result is given in Lem. 8, which is built up in the following lemmas. Consider a block index $K \in [M]$. Define the number $t_K = M \lfloor (t - K)/M \rfloor + K$ when $t - 1 \geq K$ and $t_K = 0$ otherwise.

Lemma 5. *It holds that*

$$\sum_{i \in B_K} (q_{t,i} - \hat{q}_{t-1,i})^2 \leq \sum_{i \in B_K} (t - t_K) \sum_{s=t_K+1}^t (q_{s,i} - q_{s-1,i})^2.$$

Proof. We define t_K to be the earliest time index τ on or before $t-1$ when block K of q_τ was used to update \hat{q}_τ . When $t-1 < K$, then $t_K = 0$. When $t-1 \geq K$, we can compute this number $t_K = M \lfloor [(t-1) - (K-1)]/M \rfloor + K =$

$M \lfloor (t - K)/M \rfloor + K$. Then, write

$$\begin{aligned} \sum_{i \in B_K} (q_{t,i} - \hat{q}_{t-1,i})^2 &= \sum_{i \in B_K} (q_{t,i} - q_{t_K,i})^2 \\ &= \sum_{i \in B_K} \left(\sum_{s=t_K+1}^t q_{s,i} - q_{s-1,i} \right)^2 \\ &\leq \sum_{i \in B_K} (t - t_K) \sum_{s=t_K+1}^t (q_{s,i} - q_{s-1,i})^2, \end{aligned}$$

where the last line follows by Young's inequality. \square

While we will not be able to cancel these terms on every iterate, we will be able to when aggregating over time and then redistributing them. Recall $(a_t)_{t \geq 1}$ as described in Appx. C.1. Indeed, by summing across iterations, we see that

$$\sum_{t=1}^T a_t \sum_{i=1}^n (q_{t,i} - \hat{q}_{t-1,i})^2 \leq \sum_{t=1}^T a_t \sum_{K=1}^M \sum_{i \in B_K} (t - t_K) \sum_{s=t_K+1}^t (q_{s,i} - q_{s-1,i})^2.$$

We can start by swapping the first two sums and only considering the values of t that are greater than or equal to K .

$$\begin{aligned} &\sum_{t=1}^T a_t \sum_{K=1}^M \sum_{i \in B_K} (t - t_K) \sum_{s=t_K+1}^t (q_{s,i} - q_{s-1,i})^2 \\ &= \sum_{K=1}^M \sum_{t=1}^{K-1} a_t \sum_{i \in B_K} (t - t_K) \sum_{s=t_K+1}^t (q_{s,i} - q_{s-1,i})^2 + \sum_{K=1}^M \sum_{t=K}^T a_t \sum_{i \in B_K} (t - t_K) \sum_{s=t_K+1}^t (q_{s,i} - q_{s-1,i})^2 \\ &= \underbrace{\sum_{K=1}^M \sum_{t=1}^{K-1} a_t \sum_{i \in B_K} t \sum_{s=1}^t (q_{s,i} - q_{s-1,i})^2}_{S_0} + \underbrace{\sum_{K=1}^M \sum_{t=K}^T a_t \sum_{i \in B_K} (t - t_K) \sum_{s=t_K+1}^t (q_{s,i} - q_{s-1,i})^2}_{S_1}, \end{aligned} \quad (27)$$

where we use in the last line that $t_K = 0$ when $t < K$. We handle the terms S_0 and S_1 separately. In either case, we have to match the sums over K and over i in order to create complete vectors, as opposed to differences between coordinates. We also maintain the update rules of the sequence $(a_t)_{t \geq 1}$ that will be used in the proof.

Lemma 6. *Assume that $\eta \leq \frac{1}{M}$ and $a_t \leq (1 + \eta)a_{t-1}$. It holds that S_0 as defined in (27) satisfies*

$$S_0 \leq \frac{eM(M-1)}{2} \sum_{t=1}^{M-1} a_t \|q_t - q_{t-1}\|_2^2.$$

Proof. Write

$$\begin{aligned}
S_0 &= \sum_{K=1}^M \sum_{t=1}^{K-1} a_t \sum_{i \in B_K} t \sum_{s=1}^t (q_{s,i} - q_{s-1,i})^2 && \text{by definition} \\
&= \sum_{t=1}^{M-1} t a_t \sum_{K=t+1}^M \sum_{i \in B_K} \sum_{s=1}^t (q_{s,i} - q_{s-1,i})^2 && \text{swap sums over } K \text{ and } t \\
&= \sum_{t=1}^{M-1} t a_t \sum_{s=1}^t \sum_{K=t+1}^M \sum_{i \in B_K} (q_{s,i} - q_{s-1,i})^2 && \text{move sum over } s \\
&\leq \sum_{t=1}^{M-1} t a_t \sum_{s=1}^t \sum_{K=1}^M \sum_{i \in B_K} (q_{s,i} - q_{s-1,i})^2 && \sum_{K=t+1}^M (\cdot) \leq \sum_{K=1}^M (\cdot) \\
&= \sum_{t=1}^{M-1} t a_t \sum_{s=1}^t \|q_s - q_{s-1}\|_2^2 && \sum_{K=1}^M \sum_{i \in B_K} (\cdot) = \sum_{i=1}^n (\cdot) \\
&= \sum_{s=1}^{M-1} \left(\sum_{t=s}^{M-1} t a_t \right) \|q_s - q_{s-1}\|_2^2 && \text{swap sums over } s \text{ and } t \\
&\leq \sum_{s=1}^{M-1} \left(\sum_{t=s}^{M-1} t (1 + \eta)^{t-s} a_s \right) \|q_s - q_{s-1}\|_2^2 && a_t \leq (1 + \eta) a_{t-1} \\
&\leq \sum_{s=1}^{M-1} a_s (1 + \eta)^M \left(\sum_{t=s}^{M-1} t \right) \|q_s - q_{s-1}\|_2^2 && t - s \leq M \\
&\leq \sum_{s=1}^{M-1} e a_s \left(\sum_{t=s}^{M-1} t \right) \|q_s - q_{s-1}\|_2^2 && \eta \leq \frac{1}{M} \implies (1 + \eta)^M \leq e \\
&\leq \sum_{s=1}^{M-1} e a_s \left(\sum_{t=1}^{M-1} t \right) \|q_s - q_{s-1}\|_2^2 && \sum_{t=s}^{M-1} (\cdot) \leq \sum_{t=1}^{M-1} (\cdot) \\
&= \frac{eM(M-1)}{2} \sum_{s=1}^{M-1} a_s \|q_s - q_{s-1}\|_2^2,
\end{aligned}$$

the result as desired. \square

Thus, S_0 contributes about M^3 of such terms over the entire trajectory, which can be viewed as an initialization cost. Next, we control S_1 .

Lemma 7. *Assume that $\eta \leq \frac{1}{M}$ and $a_t \leq (1 + \eta)a_{t-1}$. It holds that S_1 as defined in (27) satisfies*

$$S_1 \leq 2e^2 M^2 \sum_{t=1}^T a_t \|q_t - q_{t-1}\|_2^2.$$

Proof. We can reparametrize t in terms of $r = t - K$, which will help in reasoning with t_K . Define $r_K = M \lfloor r/M \rfloor +$

K , and let

$$\begin{aligned}
S_1 &= \sum_{K=1}^M \sum_{r=0}^{T-K} a_{r+K} \sum_{i \in B_K} (r+K-r_K) \sum_{s=r_K+1}^{r+K} (q_{s,i} - q_{s-1,i})^2 && \text{by definition and } r = t - K \\
&\leq M \sum_{K=1}^M \sum_{r=0}^{T-K} a_{r+K} \sum_{i \in B_K} \sum_{s=r_K+1}^{r+K} (q_{s,i} - q_{s-1,i})^2 && (r - M \lfloor r/M \rfloor) \leq M \\
&\leq M \sum_{K=1}^M \sum_{r=0}^{T-K} (1+\eta)^K a_r \sum_{i \in B_K} \sum_{s=r_K+1}^{r+K} (q_{s,i} - q_{s-1,i})^2 && a_t \leq (1+\eta)a_{t-1} \\
&\leq eM \sum_{K=1}^M \sum_{r=0}^{T-K} a_r \sum_{i \in B_K} \sum_{s=r_K+1}^{r+K} (q_{s,i} - q_{s-1,i})^2 && K \leq M \text{ and } \eta \leq \frac{1}{M} \\
&= eM \sum_{r=0}^{T-2} a_r \sum_{K=1}^{\min\{T-r, M\}} \sum_{i \in B_K} \sum_{s=r_K+1}^{r+K} (q_{s,i} - q_{s-1,i})^2 && \text{swap sums over } r \text{ and } K \\
&\leq eM \sum_{r=0}^{T-2} a_r \sum_{K=1}^{\min\{T-r, M\}} \sum_{i \in B_K} \sum_{s=M \lfloor r/M \rfloor + 1}^{\min\{r+M, T\}} (q_{s,i} - q_{s-1,i})^2 && \sum_{s=r_K+1}^{r+K} (\cdot) \leq \sum_{s=M \lfloor r/M \rfloor + 1}^{\min\{r+M, T\}} (\cdot) \\
&= eM \sum_{r=0}^{T-2} a_r \sum_{s=M \lfloor r/M \rfloor + 1}^{\min\{r+M, T\}} \sum_{K=1}^{\min\{T-r, M\}} \sum_{i \in B_K} (q_{s,i} - q_{s-1,i})^2 && \text{move sum over } s \\
&\leq eM \sum_{r=0}^{T-2} a_r \sum_{s=M \lfloor r/M \rfloor + 1}^{\min\{r+M, T\}} \sum_{K=1}^M \sum_{i \in B_K} (q_{s,i} - q_{s-1,i})^2 && \sum_{K=1}^{\min\{T-r, M\}} (\cdot) \leq \sum_{K=1}^M (\cdot) \\
&= eM \sum_{r=0}^{T-2} a_r \sum_{s=M \lfloor r/M \rfloor + 1}^{\min\{r+M, T\}} \|q_s - q_{s-1}\|_2^2 && \sum_{K=1}^M \sum_{i \in B_K} (\cdot) = \sum_{i=1}^n (\cdot) \\
&\leq eM \sum_{r=0}^{T-2} \sum_{s=M \lfloor r/M \rfloor}^{\min\{r+M, T\}} (1+\eta)^{r-s} a_s \|q_s - q_{s-1}\|_2^2 && a_t \leq (1+\eta)a_{t-1} \\
&\leq e^2 M \sum_{r=0}^{T-2} \sum_{s=M \lfloor r/M \rfloor}^{\min\{r+M, T\}} a_s \|q_s - q_{s-1}\|_2^2 && r - s \leq M \text{ and } \eta \leq \frac{1}{M} \\
&\leq 2e^2 M^2 \sum_{s=1}^{T-1} a_s \|q_s - q_{s-1}\|_2^2.
\end{aligned}$$

The last line follows because the inner sum $\sum_{s=M \lfloor r/M \rfloor}^{\min\{r+M, T\}} a_s \|q_s - q_{s-1}\|_2^2$ can be thought of as a sliding window of size at most $2M$ centered at r , which essentially repeats each element in the sum $2M$ times at most. \square

In either case, the contribution over the entire trajectory is order $M^2 = (n/b)^2$ terms. Combining the bounds for S_0 and S_1 yields the following.

Lemma 8. *Letting $M = n/b$ be the number of blocks. Assume that $\eta \leq \frac{1}{M}$ and $a_t \leq (1+\eta)a_{t-1}$. We have that*

$$\sum_{t=1}^T a_t \sum_{i=1}^n (q_{t,i} - \hat{q}_{t-1,i})^2 \leq 3e^2 M^2 \sum_{t=1}^T a_t \|q_t - q_{t-1}\|_2^2.$$

Proof. Use Lem. 5 to achieve (27) and apply Lem. 6 and Lem. 7 on each term to get

$$\begin{aligned} \sum_{t=1}^T a_t \sum_{i=1}^n (q_{t,i} - \hat{q}_{t-1,i})^2 &\leq \frac{eM(M-1)}{2} \sum_{t=1}^{M-1} a_t \|q_t - q_{t-1}\|_2^2 + 2e^2 M^2 \sum_{t=1}^T a_t \|q_t - q_{t-1}\|_2^2 \\ &\leq 3e^2 M^2 \sum_{t=1}^T a_t \|q_t - q_{t-1}\|_2^2, \end{aligned}$$

completing the proof. \square

We close this subsection with comments on how Lem. 8 can be used. The term $\mathbb{E}_t \|\delta_t^D\|_2^2$ is multiplied in (32) by a factor $\frac{na_{t-1}^2 G^2}{\mu C_{t-1}}$. Thus, if we apply Lem. 8 when redistributing over time a term $\|q_{t-1} - q_{t-2}\|_2^2$ which will be multiplied by a factor (ignoring absolute constants) of

$$\frac{na_{t-1}^2 G^2}{\mu C_{t-1}} \cdot M^2 = \frac{n^3 a_{t-1}^2 G^2}{b^2 \mu C_{t-1}}.$$

In order to cancel such a term, we require the use of $-\frac{A_{t-1}\nu}{2} \|q_t - q_{t-1}\|_2^2$. We can reserve half to be used up by (45), and be left with the condition

$$\frac{n^3 a_{t-1}^2 G^2}{b^2 \mu C_{t-1}} \leq A_{t-1}\nu \iff \alpha^2 \leq \frac{b^2}{n^2} \frac{\mu\nu}{2nG^2},$$

as we have applied that $a_{t-1} \leq 2\alpha C_{t-1}$ and $a_{t-1} \leq \alpha A_{t-1}$. Thus, this introduces a dependence of order $\frac{n}{b} \sqrt{\frac{nG^2}{\mu\nu}}$ on α , which propagates to the learning rate η . We now proceed to the main logic of the convergence analysis.

C.3 Proof of Main Result

C.3.1 Lower Bound on Dual Objective

We first quantify the gap between $\mathcal{L}(w_*, q_t)$ and $\mathcal{L}(w_*, q_*)$ by providing a lower bound in expectation on $\mathcal{L}(w_*, q_t)$, given in Lem. 9. As in Lem. 3, recall the notation $\pi(t, i)$ to satisfy $\hat{q}_{t,i} = q_{\pi(t,i),i}$ and $g_{t,i} = \nabla \ell_i(w_{\pi(t,i)})$, that is, the time index of the last update of table element i on or before time t , with $\pi(t, i) = 0$ for $t \leq 0$.

Lemma 9. *Assume that $\alpha \leq \mu/(24eLnq_{\max})$. Then, for $t \geq 2$, we have that:*

$$\begin{aligned} & - \mathbb{E}_t [a_t \mathcal{L}(w_*, q_t)] \\ & \leq -a_t \mathbb{E}_t [q_t^\top \ell(w_t)] - \frac{a_t}{2L} \sum_{i=1}^n q_{t,i} \mathbb{E}_t \|\nabla \ell_i(w_t) - \nabla \ell_i(w_*)\|_2^2 \\ & \quad + \frac{a_{t-1}}{4L} \sum_{i=1}^n q_{t-1,i} \|\nabla \ell_i(w_{t-1}) - \nabla \ell_i(w_*)\|_2^2 + \sum_{i=1}^n \frac{a_{\pi(t-2,i)}}{4L} q_{\pi(t-2,i),i} \|\nabla \ell_i(w_{\pi(t-2,i)} - \nabla \ell_i(w_*)\|_2^2 \\ & \quad + \frac{6n\alpha a_{t-1} G^2}{\mu} \|q_{t-1} - \hat{q}_{t-2}\|_2^2 \\ & \quad - a_t \mathbb{E}_t [\langle \nabla \ell(w_t)^\top q_t - \hat{g}_{t-1}^\top \hat{q}_{t-1}, w_* - w_t \rangle] + a_{t-1} \langle \nabla \ell(w_{t-1})^\top q_{t-1} - \hat{g}_{t-2}^\top \hat{q}_{t-2}, w_* - w_{t-1} \rangle \\ & \quad - \frac{a_t \mu}{2} \mathbb{E}_t \|w_t\|_2^2 + a_t \nu \mathbb{E}_t [D(q_t | q_0)] - \frac{\mu A_t}{2} \mathbb{E}_t \|w_* - w_t\|_2^2 \\ & \quad - \frac{\mu C_{t-1}}{4} \|w_t - w_{t-1}\|_2^2 + \frac{\mu C_{t-1}}{2} \|w_* - w_{t-1}\|_2^2 \\ & \quad - \frac{c_{t-1} \mu}{2} \sum_{\tau=t-n/b}^{t-2} \mathbb{E}_t \|w_t - w_{\tau \vee 0}\|_2^2 + \frac{c_{t-1} \mu}{2} \sum_{\tau=t-n/b}^{t-2} \|w_* - w_{\tau \vee 0}\|_2^2. \end{aligned}$$

Proof. We use **convexity and smoothness (1)**, then **add and subtract (2)** elements from the primal update, and finally use the definition of the **proximal operator (3)** with the optimality of w_t for the problem that defines it.

$$\begin{aligned}
a_t \mathcal{L}(w_*, q_t) &:= a_t q_t^\top \ell(w_*) + a_t \frac{\mu}{2} \|w_*\|_2^2 - a_t \nu D(q_t \| q_0) \\
&\stackrel{(1)}{\geq} a_t q_t^\top \ell(w_t) + a_t \langle \nabla \ell(w_t)^\top q_t, w_* - w_t \rangle + \frac{a_t}{2L} \sum_{i=1}^n q_{t,i} \|\nabla \ell_i(w_t) - \nabla \ell_i(w_*)\|_2^2 \\
&\quad + \frac{a_t \mu}{2} \|w_*\|_2^2 - \nu D(q_t \| q_0) \\
&\stackrel{(2)}{=} a_t q_t^\top \ell(w_t) + a_t \langle \nabla \ell(w_t)^\top q_t - v_t^P, w_* - w_t \rangle + a_t \langle v_t^P, w_* - w_t \rangle \\
&\quad + \frac{a_t \mu}{2} \|w_*\|_2^2 - a_t \nu D(q_t \| q_0) + \frac{a_t}{2L} \sum_{i=1}^n q_{t,i} \|\nabla \ell_i(w_t) - \nabla \ell_i(w_*)\|_2^2 \\
&\quad + \frac{\mu C_{t-1}}{2} \|w_* - w_{t-1}\|_2^2 - \frac{\mu C_{t-1}}{2} \|w_* - w_{t-1}\|_2^2 \\
&\quad + \frac{c_{t-1} \mu}{2} \sum_{\tau=t-n/b}^{t-2} \|w_* - w_{\tau \vee 0}\|_2^2 - \frac{c_{t-1} \mu}{2} \sum_{\tau=t-n/b}^{t-2} \|w_* - w_{\tau \vee 0}\|_2^2 \\
&\stackrel{(3)}{\geq} a_t q_t^\top \ell(w_t) + a_t \underbrace{\langle \nabla \ell(w_t)^\top q_t - v_t^P, w_* - w_t \rangle}_{\text{cross term}} + a_t \underbrace{\langle v_t^P, w_* - w_t \rangle}_{=0} \\
&\quad + \frac{a_t \mu}{2} \|w_t\|_2^2 - a_t \nu D(q_t \| q_0) + \frac{a_t}{2L} \sum_{i=1}^n q_{t,i} \|\nabla \ell_i(w_t) - \nabla \ell_i(w_*)\|_2^2 \\
&\quad + \frac{\mu C_{t-1}}{2} \|w_t - w_{t-1}\|_2^2 - \frac{\mu C_{t-1}}{2} \|w_* - w_{t-1}\|_2^2 \\
&\quad + \frac{c_{t-1} \mu}{2} \sum_{\tau=t-n/b}^{t-2} \|w_t - w_{\tau \vee 0}\|_2^2 - \frac{c_{t-1} \mu}{2} \sum_{\tau=t-n/b}^{t-2} \|w_* - w_{\tau \vee 0}\|_2^2 \\
&\quad + \frac{\mu A_t}{2} \|w_* - w_t\|_2^2.
\end{aligned} \tag{28}$$

Next, we are able to use Lem. 2 with $v_t = v_t^P$, $y_t = \nabla \ell(w_t)^\top q_t$, $\hat{y}_t = \hat{g}_t^\top \hat{q}_t$, $x_t = w_t$, $x_* = w_*$, and $\gamma = \mu C_{t-1}/2$ which yields that

$$\begin{aligned}
&a_t \mathbb{E}_t [\langle \nabla \ell(w_t)^\top q_t - v_t^P, w_* - w_t \rangle] \\
&\leq a_t \mathbb{E}_t [\langle \nabla \ell(w_t)^\top q_t - \hat{g}_{t-1}^\top \hat{q}_{t-1}, w_* - w_t \rangle] - a_{t-1} \langle \nabla \ell(w_{t-1})^\top q_{t-1} - \hat{g}_{t-2}^\top \hat{q}_{t-2}, w_* - w_{t-1} \rangle \\
&\quad + \frac{n^2 a_{t-1}^2}{\mu C_{t-1}} \underbrace{\mathbb{E}_t \left[\left\| \frac{1}{b} \sum_{i \in I_t} \nabla \ell_i(w_{t-1}) q_{t-1,i} - g_{t-2,i} \hat{q}_{t-2,i} \right\|_2^2 \right]}_{\mathbb{E}_t \|\delta_t^P\|_2^2} + \frac{\mu C_{t-1}}{4} \mathbb{E}_t \|w_t - w_{t-1}\|_2^2.
\end{aligned} \tag{31}$$

Then, apply Lem. 3 to achieve

$$\begin{aligned}
\mathbb{E}_t \|\delta_t^P\|_2^2 &\leq \frac{3q_{\max}}{n} \sum_{i=1}^n q_{t-1,i} \|\nabla \ell_i(w_{t-1}) - \nabla \ell_i(w_*)\|_2^2 \\
&\quad + \frac{3q_{\max}}{n} \sum_{i=1}^n q_{\pi(t-2,i),i} \|\nabla \ell_i(w_{\pi(t-2,i)}) - \nabla \ell_i(w_*)\|_2^2 \\
&\quad + \frac{3G^2}{n} \|q_{t-1} - \hat{q}_{t-2}\|_2^2
\end{aligned} \tag{32}$$

In the following, the blue terms indicate what changes from line to line. Combine the previous two steps to collect all

terms for the lower bound. That is, apply (30) to write

$$\begin{aligned}
& \mathbb{E}_t[a_t \mathcal{L}(w_\star, q_t)] \\
& := a_t q_t^\top \ell(w_\star) + a_t \frac{\mu}{2} \|w_\star\|_2^2 - a_t \nu D(q_t \| q_0) \\
& \geq a_t q_t^\top \ell(w_t) + \mathbb{E}_t[a_t \langle \nabla \ell(w_t)^\top q_t - v_t^P, w_\star - w_t \rangle] + \frac{a_t}{2L} \sum_{i=1}^n q_{t,i} \|\nabla \ell_i(w_t) - \nabla \ell_i(w_\star)\|_2^2 \\
& \quad + \frac{a_t \mu}{2} \|w_t\|_2^2 - a_t \nu D(q_t \| q_0) + \frac{\mu A_t}{2} \|w_\star - w_t\|_2^2 \\
& \quad + \frac{\mu C_{t-1}}{2} \|w_t - w_{t-1}\|_2^2 - \frac{\mu C_{t-1}}{2} \|w_\star - w_{t-1}\|_2^2 \\
& \quad + \frac{c_{t-1} \mu}{2} \sum_{\tau=t-n/b}^{t-2} \|w_t - w_{\tau \vee 0}\|_2^2 - \frac{c_{t-1} \mu}{2} \sum_{\tau=t-n/b}^{t-2} \|w_\star - w_{\tau \vee 0}\|_2^2,
\end{aligned}$$

then apply (31) to the blue term above to write

$$\begin{aligned}
& \mathbb{E}_t[a_t \mathcal{L}(w_\star, q_t)] \\
& \geq a_t q_t^\top \ell(w_t) + \frac{a_t}{2L} \sum_{i=1}^n q_{t,i} \|\nabla \ell_i(w_t) - \nabla \ell_i(w_\star)\|_2^2 \\
& \quad - \frac{n^2 a_{t-1}^2}{\mu C_{t-1}} \mathbb{E}_t \|\nabla \ell_{i_{t-1}}(w_{t-1}) q_{t-1, i_{t-1}} - g_{t-2, i_{t-1}} \hat{q}_{t-2, i_{t-1}}\|_2^2 \\
& \quad + a_t \mathbb{E}_t [\langle \nabla \ell(w_t)^\top q_t - \hat{g}_{t-1}^\top \hat{q}_{t-1}, w_\star - w_t \rangle] - a_{t-1} \langle \nabla \ell(w_{t-1})^\top q_{t-1} - \hat{g}_{t-2}^\top \hat{q}_{t-2}, w_\star - w_{t-1} \rangle \\
& \quad + \frac{a_t \mu}{2} \|w_t\|_2^2 - a_t \nu D(q_t \| q_0) + \frac{\mu A_t}{2} \|w_\star - w_t\|_2^2 \\
& \quad + \frac{\mu C_{t-1}}{4} \|w_t - w_{t-1}\|_2^2 - \frac{\mu C_{t-1}}{2} \|w_\star - w_{t-1}\|_2^2 \\
& \quad + \frac{c_{t-1} \mu}{2} \sum_{\tau=t-n/b}^{t-2} \|w_t - w_{\tau \vee 0}\|_2^2 - \frac{c_{t-1} \mu}{2} \sum_{\tau=t-n/b}^{t-2} \|w_\star - w_{\tau \vee 0}\|_2^2.
\end{aligned} \tag{33}$$

Finally, apply (32) to the term (33) to achieve

$$\begin{aligned}
& \geq a_t q_t^\top \ell(w_t) + \frac{a_t}{2L} \sum_{i=1}^n q_{t,i} \|\nabla \ell_i(w_t) - \nabla \ell_i(w_\star)\|_2^2 \\
& \quad - \frac{3nq_{\max} a_{t-1}^2}{\mu C_{t-1}} \sum_{i=1}^n q_{t-1, i} \|\nabla \ell_i(w_{t-1}) - \nabla \ell_i(w_\star)\|_2^2 - \frac{3nq_{\max} a_{t-1}^2}{\mu C_{t-1}} \sum_{i=1}^n q_{\pi(t-2, i), i} \|\nabla \ell_i(w_{\pi(t-2, i)}) - \nabla \ell_i(w_\star)\|_2^2 \\
& \quad - \frac{3nG^2 a_{t-1}^2}{\mu C_{t-1}} \|q_{t-1} - \hat{q}_{t-2}\|_2^2 \\
& \quad + a_t \mathbb{E}_t [\langle \nabla \ell(w_t)^\top q_t - \hat{g}_{t-1}^\top \hat{q}_{t-1}, w_\star - w_t \rangle] - a_{t-1} \langle \nabla \ell(w_{t-1})^\top q_{t-1} - \hat{g}_{t-2}^\top \hat{q}_{t-2}, w_\star - w_{t-1} \rangle \\
& \quad + \frac{a_t \mu}{2} \|w_t\|_2^2 - a_t \nu D(q_t \| q_0) + \frac{\mu A_t}{2} \|w_\star - w_t\|_2^2 \\
& \quad + \frac{\mu C_{t-1}}{4} \|w_t - w_{t-1}\|_2^2 - \frac{\mu C_{t-1}}{2} \|w_\star - w_{t-1}\|_2^2 \\
& \quad + \frac{c_{t-1} \mu}{2} \sum_{\tau=t-n/b}^{t-2} \|w_t - w_{\tau \vee 0}\|_2^2 - \frac{c_{t-1} \mu}{2} \sum_{\tau=t-n/b}^{t-2} \|w_\star - w_{\tau \vee 0}\|_2^2.
\end{aligned}$$

Next, we apply $a_{t-1} \leq 2\alpha C_{t-1}$ and $\alpha \leq \frac{\mu}{24eLnq_{\max}}$ to achieve:

$$\begin{aligned}\frac{3nG^2 a_{t-1}^2}{\mu C_{t-1}} &\leq \frac{6nG^2 \alpha a_{t-1}}{\mu}, \\ \frac{3nq_{\max} a_{t-1}^2}{\mu C_{t-1}} &\leq \frac{a_{t-1}}{4L}, \\ \frac{3nq_{\max} a_{t-1}^2}{\mu C_{t-1}} &\leq \frac{a_{\pi(t-2,i)}}{4L}, \quad \forall i \in [n]\end{aligned}$$

For terms that contain $\pi(t-2, i)$, we recall that $\pi(t-2, i)$ can be at most n/b timesteps behind $t-2$, so we have that

$$a_{t-1} \leq \left(1 + \frac{1}{n/b}\right)^{n/b} a_{t-n/b} \leq e a_{t-n/b} \leq e a_{\pi(t-2,i)}.$$

We use here that $a_t \leq (1 + \frac{\alpha}{4})a_{t-1}$ and impose the condition $\frac{\alpha}{4} \leq \frac{b}{n}$ in the rate. Substituting this back into the lower bound achieves the desired claim. \square

C.3.2 Upper Bound on Gap Criterion

Next, we quantify the gap between $\mathcal{L}(w_t, q_*)$ and $\mathcal{L}(w_*, q_*)$ by upper bounding $a_t \mathcal{L}(w_t, q_*)$, as given in Lem. 10. When combined with the lower bound Lem. 9, we may then control the gap.

Lemma 10. *For $t \geq 2$, we have that:*

$$\begin{aligned}a_t \mathcal{L}(w_t, q_*) &\leq a_t q_*^\top (\ell(w_t) - v_t^D) + \frac{a_t \mu}{2} \|w_t\|_2^2 + A_{t-1} \nu \Delta_D(q_*, q_{t-1}) \\ &\quad + a_t q_t^\top v_t^D - a_t \nu D(q_t \| q_0) - A_{t-1} \nu \Delta_D(q_t, q_{t-1}) - A_t \nu \Delta_D(q_*, q_t).\end{aligned}$$

Proof. We add and subtract (1) terms in the dual update step and apply the definition of the proximal operator (2) with Bregman divergence, and the optimality of q_t for the maximization problem that defines it.

$$\begin{aligned}a_t \mathcal{L}(w_t, q_*) &:= a_t q_*^\top \ell(w_t) - a_t \nu D(q_* \| q_0) + \frac{a_t \mu}{2} \|w_t\|_2^2 \\ &\stackrel{(1)}{=} a_t q_*^\top (\ell(w_t) - v_t^D) + \frac{a_t \mu}{2} \|w_t\|_2^2 + A_{t-1} \nu \Delta_D(q_*, q_{t-1}) \\ &\quad + a_t q_*^\top v_t^D - a_t \nu D(q_* \| q_0) - A_{t-1} \nu \Delta_D(q_*, q_{t-1}) \\ &\stackrel{(2)}{\leq} a_t q_*^\top (\ell(w_t) - v_t^D) + \frac{a_t \mu}{2} \|w_t\|_2^2 + A_{t-1} \nu \Delta_D(q_*, q_{t-1}) \\ &\quad + a_t q_t^\top v_t^D - a_t \nu D(q_t \| q_0) - A_{t-1} \nu \Delta_D(q_t, q_{t-1}) - A_t \nu \Delta_D(q_*, q_t).\end{aligned}$$

\square

We can combine the upper bound from Lem. 10 and lower bound from Lem. 9 in Lem. 11. We identify telescoping terms in blue and non-positive terms in red. The green term is canceled after aggregation across time t . This bound, like before applies for $t \geq 2$.

Lemma 11. Assume that $\alpha \leq \mu/(24eLnq_{\max})$. For $t > 2$, we have that:

$$\begin{aligned} \mathbb{E}_t[\gamma_t] &= \mathbb{E}_t \left[a_t(\mathcal{L}(w_t, q_\star) - \mathcal{L}(w_\star, q_t) - \frac{a_t\mu}{2} \|w_t - w_\star\|_2^2 - \frac{a_t\nu}{2} \|q_t - q_\star\|_2^2) \right] \\ &\leq a_t \mathbb{E}_t \left[(q_\star - q_t)^\top (\ell(w_t) - \hat{\ell}_t) \right] - a_{t-1} (q_\star - q_{t-1})^\top (\ell(w_{t-1}) - \hat{\ell}_{t-1}) \end{aligned} \quad (34)$$

$$+ A_{t-1}\nu\Delta_D(q_\star, q_{t-1}) - A_t\nu\mathbb{E}_t[\Delta_D(q_\star, q_t)] \quad (35)$$

$$- \frac{a_t}{2L} \mathbb{E}_t \left[\sum_{i=1}^n q_{t,i} \|\nabla\ell_i(w_t) - \nabla\ell_i(w_\star)\|_2^2 \right] \quad (36)$$

$$+ \frac{a_{t-1}}{4L} \sum_{i=1}^n q_{t-1,i} \|\nabla\ell_i(w_{t-1}) - \nabla\ell_i(w_\star)\|_2^2 + \sum_{i=1}^n \frac{a_{\pi(t-2,i)}}{4L} q_{\pi(t-2,i)} \|\nabla\ell_i(w_{\pi(t-2,i)} - \nabla\ell_i(w_\star))\|_2^2 \quad (37)$$

$$- a_t \mathbb{E}_t \left[\langle \nabla\ell(w_t)^\top q_t - \hat{g}_{t-1}^\top \hat{q}_{t-1}, w_\star - w_t \rangle \right] + a_{t-1} \langle \nabla\ell(w_{t-1})^\top q_{t-1} - \hat{g}_{t-2}^\top \hat{q}_{t-2}, w_\star - w_{t-1} \rangle \quad (38)$$

$$+ \frac{6nG^2\alpha a_{t-1}}{\mu} \|q_{t-1} - \hat{q}_{t-2}\|_2^2 \quad (39)$$

$$- \frac{\mu A_t}{2} \mathbb{E}_t \|w_\star - w_t\|_2^2 + \frac{\mu C_{t-1}}{2} \|w_\star - w_{t-1}\|_2^2 + \frac{c_{t-1}\mu}{2} \sum_{\tau=t-n/b}^{t-2} \|w_\star - w_{\tau\nu 0}\|_2^2 \quad (40)$$

$$+ \frac{na_{t-1}\alpha G^2}{\nu} \sum_{\tau=t-n/b}^{t-3} \|w_{t-1} - w_{\tau\nu 0}\|_2^2 - \frac{c_{t-1}\mu}{2} \sum_{\tau=t-n/b}^{t-2} \mathbb{E}_t \|w_t - w_{\tau\nu 0}\|_2^2 \quad (41)$$

$$+ \frac{na_{t-1}\alpha G^2}{\nu} \|w_{t-1} - w_{t-2}\|_2^2 - \frac{\mu C_{t-1}}{4} \mathbb{E}_t \|w_t - w_{t-1}\|_2^2 \quad (42)$$

$$- \frac{a_t\mu}{2} \mathbb{E}_t \left[\|w_t - w_\star\|_2^2 \right] - \frac{a_t\nu}{2} \mathbb{E}_t \|q_t - q_\star\|_2^2 - \frac{A_{t-1}\nu}{2} \mathbb{E}_t [\Delta_D(q_t, q_{t-1})]. \quad (43)$$

For $t = 2$, the above holds with the addition of the term $\frac{nG^2}{\nu\mu^2} \|\nabla\ell(w_0)^\top q_0\|_2^2$.

Proof. First, combine Lem. 9 and Lem. 10 to write:

$$\begin{aligned} \mathbb{E}_t[\gamma_t] &= \mathbb{E}_t \left[a_t(\mathcal{L}(w_t, q_\star) - \mathcal{L}(w_\star, q_t) - \frac{a_t\mu}{2} \|w_t - w_\star\|_2^2 - \frac{a_t\nu}{2} \|q_t - q_\star\|_2^2) \right] \\ &\leq \underbrace{\mathbb{E}_t \left[a_t(q_\star - q_t)^\top (\ell(w_t) - v_t^D) \right]}_{\text{cross term}} \\ &\quad + \mathbb{E}_t \left[A_{t-1}\nu\Delta_D(q_\star, q_{t-1}) - A_t\nu\Delta_D(q_\star, q_t) \right] \\ &\quad - \mathbb{E}_t \left[\frac{a_t}{2L} \sum_{i=1}^n q_{t,i} \|\nabla\ell_i(w_t) - \nabla\ell_i(w_\star)\|_2^2 \right] \\ &\quad + \frac{a_{t-1}}{4L} \sum_{i=1}^n q_{t-1,i} \|\nabla\ell_i(w_{t-1}) - \nabla\ell_i(w_\star)\|_2^2 + \sum_{i=1}^n \frac{a_{\pi(t-2,i)}}{4L} q_{\pi(t-2,i)} \|\nabla\ell_i(w_{\pi(t-2,i)} - \nabla\ell_i(w_\star))\|_2^2 \\ &\quad + \frac{6nG^2\alpha a_{t-1}}{\mu} \|q_{t-1} - \hat{q}_{t-2}\|_2^2 \\ &\quad - a_t \mathbb{E}_t \left[\langle \nabla\ell(w_t)^\top q_t - \hat{g}_{t-1}^\top \hat{q}_{t-1}, w_\star - w_t \rangle \right] + a_{t-1} \langle \nabla\ell(w_{t-1})^\top q_{t-1} - \hat{g}_{t-2}^\top \hat{q}_{t-2}, w_\star - w_{t-1} \rangle \\ &\quad - \frac{\mu A_t}{2} \mathbb{E}_t \|w_\star - w_t\|_2^2 + \frac{\mu C_{t-1}}{2} \|w_\star - w_{t-1}\|_2^2 + \frac{c_{t-1}\mu}{2} \sum_{\tau=t-n/b}^{t-2} \|w_\star - w_{\tau\nu 0}\|_2^2 \\ &\quad - \frac{\mu C_{t-1}}{4} \mathbb{E}_t \|w_t - w_{t-1}\|_2^2 - A_{t-1}\nu\mathbb{E}_t[\Delta_D(q_t, q_{t-1})] \\ &\quad - \frac{a_t\mu}{2} \mathbb{E}_t \left[\|w_t - w_\star\|_2^2 \right] - \frac{c_{t-1}\mu}{2} \sum_{\tau=t-n/b}^{t-2} \mathbb{E}_t \|w_t - w_{\tau\nu 0}\|_2^2 - \frac{a_t\nu}{2} \mathbb{E}_t \left[\|q_t - q_\star\|_2^2 \right]. \end{aligned}$$

Bound the cross term identified above. In the case that $t = 2$, use Lem. 2 with $v_t = v_t^D$, $y_t = \ell(w_t)$, $\hat{y}_{t+1} = \hat{\ell}_t$, $x_t = q_t$, $x_\star = q_\star$, and $\gamma = \nu A_{t-1} = \nu$ which yields that

$$\begin{aligned} & a_t \mathbb{E}_t [(q_\star - q_2)^\top (\ell(w_2) - v_2^D)] \\ & \leq a_2 \mathbb{E}_2 [(q_\star - q_2)^\top (\ell(w_t) - \hat{\ell}_2)] - a_1 (q_\star - q_1)^\top (\ell(w_1) - \hat{\ell}_1) \\ & \quad + \frac{\nu}{4} \mathbb{E}_t [\|q_1 - q_0\|_2^2] + \frac{n^2}{\nu} \mathbb{E}_2 \left\| \frac{1}{b} \sum_{j \in J_t} (\ell_j(w_1) - \hat{\ell}_{1,j}) e_j \right\|_2^2, \end{aligned} \quad (44)$$

where the fourth term above can be bounded as

$$\frac{n^2}{\nu} \mathbb{E}_2 \left\| \frac{1}{b} \sum_{j \in J_t} (\ell_j(w_1) - \hat{\ell}_{1,j}) e_j \right\|_2^2 \leq \frac{nb}{\nu} \left\| \frac{1}{b} \sum_{j=1}^b (\ell_j(w_1) - \hat{\ell}_{1,j}) e_j \right\|_2^2 \leq \frac{nG^2}{\nu} \|w_1 - w_0\|.$$

Using the definition of the update, we have that $\|w_1 - w_0\|_2^2 = (1/\mu^2) \|\nabla \ell(w_0)^\top q_0\|_2^2$. In the case that $t > 2$, use Lem. 2 as above but instead with $\gamma = \nu A_{t-2}$ which yields that

$$\begin{aligned} & a_t \mathbb{E}_t [(q_\star - q_t)^\top (\ell(w_t) - v_t^D)] \\ & \leq a_t \mathbb{E}_t [(q_\star - q_t)^\top (\ell(w_t) - \hat{\ell}_t)] - a_{t-1} (q_\star - q_{t-1})^\top (\ell(w_{t-1}) - \hat{\ell}_{t-1}) \\ & \quad + \frac{A_{t-2}\nu}{4} \mathbb{E}_t [\|q_t - q_{t-1}\|_2^2] + \frac{n^2 a_{t-1}^2}{A_{t-2}\nu} \underbrace{\mathbb{E}_t \left\| \frac{1}{b} \sum_{j \in J_t} (\ell_j(w_{t-1}) - \hat{\ell}_{t-1,j}) e_j \right\|_2^2}_{\mathbb{E}_t \|\delta_t^D\|_2^2}. \end{aligned} \quad (45)$$

We may then apply Lem. 4 and $a_{t-1} \leq \alpha A_{t-2}$ to get that

$$\frac{n^2 a_{t-1}^2}{A_{t-2}\nu} \mathbb{E}_t \|\delta_t^D\|_2^2 \leq \frac{na_{t-1}\alpha G^2}{\nu} \sum_{\tau=t-n/b}^{t-2} \|w_{t-1} - w_{\tau \vee 0}\|_2^2. \quad (46)$$

We may use strong convexity to get the $\frac{A_{t-2}\nu}{4} \mathbb{E}_t [\|q_t - q_{t-1}\|_2^2]$ term to cancel with $-\frac{A_{t-1}\nu}{2} \Delta_D(q_t, q_{t-1})$ and that $A_{t-2} \leq A_{t-1}$ to complete the proof. \square

C.3.3 Determining Constants

In this section, we provide derivations that determine the values of the constant c_t that allow for cancellation of errors, and determine η such that (24) is satisfied. The latter is given formally in Lem. 12. We assume here that $n/b \geq 2$, which is taken as an assumption of Thm. 1.

In the statement of Lem. 11, the lines above (39) will telescope without additional conditions. For (40), we set $c_t = a_t/m$ for some parameter m . Note that this condition does not need to be checked when $n/b < 1$, as the additional sum term over τ will not be included in the update. Counting all the terms that will appear when matched on the index $t - 1$, we have the condition that

$$-\frac{a_{t-1}}{4} - A_{t-1} + C_{t-1} + \sum_{s=t+1}^{t+n/b-1} a_s/m \leq 0.$$

The first term result from the ‘‘good term’’ $-\frac{a_{t-1}\mu}{4} \|w_{t-1} - w_\star\|_2^2$ from the bottom. The rightmost term above results because $a_s \|w_\star - w_{\tau \vee 0}\|_2^2$ will have $\tau = t - 1$ when $s \in \{t + 1, \dots, t + n/b - 1\}$. We will begin by requiring that require that $a_t \leq (1 + \beta)a_{t-1}$ for all t and some $\beta > 0$, and then determine β below. The condition reads as

$$\frac{4n/b - 4 + m}{4m} a_{t-1} \geq \frac{(1 + \beta)^2}{m} \sum_{s=0}^{n/b-2} (1 + \beta)^s a_{t-1},$$

which can be summed and represented as

$$\frac{(4n/b - 4 + m)}{4} \geq (1 + \beta)^2 \frac{(1 + \beta)^{n/b-1} - 1}{\beta}.$$

Rearranging and taking a logarithm on both sides, this is the same as

$$\ln \left(\frac{\beta(4n/b - 4 + m)}{4(1 + \beta)^2} + 1 \right) \geq (n/b - 1) \log(1 + \beta). \quad (47)$$

Next, using the inequality $\frac{2x}{2+x} \leq \ln(1+x)$ with $x = \frac{\beta(4n/b-4+m)}{4(1+\beta)^2}$ which holds for all $x \geq 0$, we have

$$\ln \left(\frac{\beta(4n/b - 4 + m)}{4(1 + \beta)^2} + 1 \right) \geq \frac{2 \frac{\beta(4n/b-4+m)}{4(1+\beta)^2}}{2 + \frac{\beta(4n/b-4+m)}{4(1+\beta)^2}} = \frac{2\beta(4n/b - 4 + m)}{8(1 + \beta)^2 + \beta(4n/b - 4 + m)} \quad (48)$$

We can also apply the upper bound $\ln(x+1) \leq x$ with $x = \beta$ (which also holds for any $x \geq 0$) to write

$$(n/b - 1) \log(1 + \beta) \leq (n/b - 1)\beta,$$

which means that (47) will be satisfied (using (48)) if

$$\frac{2\beta(4n/b - 4 + m)}{8(1 + \beta)^2 + \beta(4n/b - 4 + m)} \geq (n/b - 1)\beta \quad (49)$$

$$\iff \frac{n/b - 1 + m/4}{n/b - 1} \geq (1 + \beta)^2 + (\beta/2)(n/b - 1 + m/4). \quad (50)$$

In order to satisfy the inequality, substitute $m = 4c\beta(n/b - 1)^2$ for some $c > 0$ to be determined and assume that $\beta \leq \frac{1}{n/b-1}$, so that $\beta(n/b - 1) \leq 1$. The LHS reads as

$$\frac{n/b - 1 + m/2}{n/b - 1} = 1 + c\beta(n/b - 1).$$

The RHS can be upper-bounded as

$$\begin{aligned} (1 + \beta)^2 + (\beta/2)(n/b - 1 + m/4) &= (1 + \beta)^2 + (\beta/2)(n/b - 1 + c\beta(n/b - 1)^2) \\ &\leq 1 + \beta(2 + \beta) + \beta(n/b - 1) \frac{1+c}{2}, \end{aligned}$$

which makes the inequality satisfied when

$$c \geq 2 \left(\frac{4 + 2\beta}{n/b - 1} + 1 \right),$$

so we can set $c = 16$. We now have the flexibility to control β , and the telescoping of (40) is achieved. For (41), set $\beta = \frac{\alpha}{4}$ and pass the condition of $\beta \leq 1/(n/b - 1)$ onto α , which maintains the rate (and is already satisfied when $\alpha \leq \frac{b}{n}$ and $n \geq 2$). Then, we can achieve

$$\frac{na_t \alpha G^2}{\nu} \leq \frac{\mu a_{t-1}}{m} = \frac{\mu a_{t-1}}{4\alpha(n/b - 1)^2}$$

by requiring that $\alpha \leq \frac{b\sqrt{\mu\nu}}{4n^{3/2}G}$, which achieves the telescoping of (41). Finally, to address (42), we may satisfy it if

$$\frac{na_t \alpha G^2}{\nu} \leq \frac{\mu C_{t-1}}{4}$$

which we can achieve by incorporating the condition $a_t \leq 4\alpha(n/b-1)^2 C_{t-1}$ into the update of a_t , because $\frac{na_t\alpha G^2}{\nu} \leq \frac{\mu a_t}{m}$ by the previous condition on α . Having chosen c_t , we are prepared to produce a learning rate parameter η to capture all conditions on α in one, as given in Lem. 12.

Lemma 12. *For all $t \geq 1$, we have the following.*

- Setting $c_t = a_t/[16\alpha(n/b-1)^2]$ implies that $a_t \leq 2\alpha C_t$.
- Using the update scheme

$$a_2 = 4\eta a_1, \text{ and } a_t = (1 + \eta) a_{t-1} \text{ for } t > 2,$$

when

$$\eta = \frac{1}{4} \min \left\{ \frac{b}{32n}, \frac{\mu}{24eLnq_{\max}}, \frac{b}{n} \sqrt{\frac{nG^2}{\mu\nu}} \right\}.$$

we have that (24) holds.

Proof. Noting that $m = 16\alpha(n/b-1)^2$ we confirm that

$$\begin{aligned} C_t &\geq A_{t-1}/2 \\ \Leftrightarrow A_t - \frac{1}{16\alpha(n/b-1)} a_t &\geq A_{t-1}/2 \\ \Leftrightarrow \left(1 - \frac{1}{16\alpha(n/b-1)}\right) a_t &\geq -A_{t-1}/2 \\ \Leftrightarrow 2 \left(\frac{1}{16\alpha(n/b-1)} - 1\right) a_t &\leq A_{t-1}. \end{aligned}$$

This condition is satisfied when $\alpha \leq \frac{1}{32(n/b-1)}$, so we incorporate $\alpha \leq \frac{b}{32n}$ into the rate, implying that $a_t \leq 2\alpha C_t$. This concludes the proof of the first bullet point.

Next, we show that $a_t \leq (1 + \alpha/4)a_{t-1}$ will imply that $a_t \leq \alpha A_{t-1}$, which is the second part of (24). First, we define $a_2 = \alpha a_1$ as an initialization (which also satisfies $a_2 \leq (1 + \alpha/4)a_1$ when $\alpha \leq 4/3$), and show inductively that if $a_{t-1} \leq \alpha A_{t-2}$, then $a_t \leq (1 + \alpha/4)a_{t-1} \implies a_t \leq \alpha A_{t-1}$. In the base case, $A_1 = a_1$, so the condition $a_2 = \alpha a_1$ satisfies $a_2 \leq \alpha A_1$. Next, fixing t and assuming that 1) $a_{t-1} \leq \alpha A_{t-2}$ and 2) that $a_t \leq (1 + \alpha/4)a_{t-1}$, we have that

$$\alpha A_{t-1} = \alpha(a_{t-1} + A_{t-2}) \geq (\alpha + 1)a_{t-1} \geq a_t,$$

the desired result. Finally, we consider the condition $a_t \leq 4\alpha(n/b-1)^2 C_{t-1}$, the third part of (24). We wish to show that the following inequality holds:

$$\begin{aligned} a_t \leq 4\alpha(n/b-1)^2 C_{t-1} &= 4\alpha(n/b-1)^2 \left(A_{t-1} - \frac{1}{4\alpha(n/b-1)} a_{t-1} \right) \\ &= 4\alpha(n/b-1)^2 \left(a_{t-1} + A_{t-2} - \frac{1}{4\alpha(n/b-1)} a_{t-1} \right) \end{aligned}$$

which is implied by the inequality

$$\begin{aligned} a_t &\leq 4\alpha(n/b-1)^2 \left(a_{t-1} + (1/\alpha)a_{t-1} - \frac{1}{4\alpha(n/b-1)} a_{t-1} \right) \\ &= 4(n/b-1)^2 \left(\alpha + 1 - \frac{1}{4(n/b-1)} \right) a_{t-1}. \end{aligned}$$

When $n/b \geq 2$, we have that $(1 + \alpha/4) \leq 4(n/b-1)^2 \left(\alpha + 1 - \frac{1}{4(n/b-1)} \right)$, so we require that $b \leq n/2$. Thus, our

final updates are given by

$$a_2 = 4\eta a_1 \leq (1 + \eta) a_1 \text{ and } a_t = (1 + \eta) a_{t-1} \text{ for } t > 2.$$

Because each condition was satisfied when using $a_t = (1 + \alpha/4)a_{t-1}$, we define $\eta = \alpha/4$ to achieve the claimed result. \square

C.3.4 Bound on Sum of Successive Gaps

Lem. 13 is an upper estimate for the expected sum of the gap function over T iterates. Recall that $\mathbb{E}_0[\cdot]$ the full expectation over $\{(I_t, J_t)\}_{t=1}^T$. The green term is a quantity that remain as an initialization term, whereas the blue terms have to be bounded from above. The terms directly below the blue terms account for all of the “negative $\pi(t-1, i)$ ” terms are not yet used up by the telescoping in lines (35), (36), and (37), and there are in fact between 1 and n copies of those terms in each iteration, even though we will use only 1.

Lemma 13 (Progress Bound). *Assume that*

$$\alpha \leq \min \left\{ \frac{b}{32n}, \frac{\mu}{24eLnq_{\max}}, \frac{b}{36e^2n} \sqrt{\frac{\mu\nu}{nG^2}} \right\}.$$

For any $T \geq 1$, we have that

$$\mathbb{E}_0 \left[\sum_{t=1}^T \gamma_t \right] \leq \frac{nG^2}{\nu\mu^2} \|\nabla\ell(w_0)^\top q_0\|_2^2 + a_T \mathbb{E}_0 \left[(q_\star - q_T)^\top (\ell(w_T) - \hat{\ell}_T) \right] \quad (51)$$

$$- a_T \mathbb{E}_0 \left[\langle \nabla\ell(w_T)^\top q_T - \hat{g}_{T-1}^\top \hat{q}_{T-1}, w_\star - w_T \rangle \right] \quad (52)$$

$$- \sum_{i=1}^n (n - T + \pi(T-1, i)) \frac{a_{\pi(T-1, i)}}{4L} \mathbb{E}_0 \left[q_{\pi(T-1, i)}^\top \|\nabla\ell_i(w_{\pi(T-1, i)}) - \nabla\ell_i(w_\star)\|_2^2 \right] \quad (53)$$

$$+ \frac{6nG^2\alpha}{\mu} \mathbb{E}_0 \sum_{t=1}^T a_{t-1} \|q_{t-1} - \hat{q}_{t-2}\|_2^2 - \sum_{t=1}^T \frac{A_{t-1}\nu}{2} \mathbb{E}_0 [D(q_t \| q_{t-1})] \quad (54)$$

$$- \frac{a_T}{2L} \sum_{i=1}^n \mathbb{E}_0 \left[q_{T, i}^\top \|\nabla\ell_i(w_T) - \nabla\ell_i(w_\star)\|_2^2 \right] - \frac{\mu A_T}{2} \mathbb{E}_0 \left[\|w_\star - w_T\|_2^2 \right] \quad (55)$$

$$- \frac{\mu a_{T-1}}{2[16\alpha(n/b-1)]} \sum_{\tau=T-\lceil n/b \rceil}^{T-2} \mathbb{E}_0 \left[\|w_T - w_{\tau \vee 0}\|_2^2 \right] \quad (56)$$

$$- A_T \nu \mathbb{E}_0 [D(q_\star \| q_T)] \quad (57)$$

$$- \sum_{t=1}^T \frac{a_t \mu}{4} \mathbb{E} \|w_t - w_\star\|_2^2 - \sum_{t=1}^T \frac{a_t \nu}{2} \mathbb{E}_0 \|q_t - q_\star\|_2^2. \quad (58)$$

Proof. We proceed by first deriving an upper bound on γ_1 , the gap function for $t = 1$. Note that w_1 is non-random, as $a_0 = 0$ implies that $v_0 = \nabla\ell(w_0)$. Using that w_1 is the optimum for the proximal operator that defines it, the upper bound can be written as

$$a_1 \mathcal{L}(w_1, q_\star) \leq a_1 q_\star^\top (\ell(w_1) - \hat{\ell}_1) + \frac{a_1 \mu}{2} \|w_1\|_2^2 + a_1 q_1^\top \hat{\ell}_1 - a_1 \nu D(q_1 \| q_0) - A_1 \nu \Delta_D(q_\star, q_1),$$

where we use that $\tilde{\ell}_1 = \hat{\ell}_1$. For the lower bound, use a similar argument to Lem. 9 to achieve

$$\begin{aligned} a_1 \mathcal{L}(w_*, q_1) &\geq a_1 q_1^\top \ell(w_1) + a_1 \langle \nabla \ell(w_1)^\top q_1 - \nabla \ell(w_0)^\top q_0, w_* - w_1 \rangle + \frac{a_1 \mu}{2} \|w_1\|_2^2 \\ &\quad - a_1 \nu D(q_1 \| q_0) + \frac{a_1}{2L} \sum_{i=1}^n q_{1,i} \|\nabla \ell_i(w_1) - \nabla \ell_i(w_*)\|_2^2 + \frac{\mu A_1}{2} \|w_* - w_1\|_2^2, \end{aligned}$$

where we use that $v_0^P = \nabla \ell(w_0)^\top q_0$. We combine them to get

$$\begin{aligned} \gamma_1 &\leq a_1 (q_* - q_1)^\top (\ell(w_1) - \hat{\ell}_1) - a_1 \langle \nabla \ell(w_1)^\top q_1 - \nabla \ell(w_0)^\top q_0, w_* - w_1 \rangle \\ &\quad - \frac{a_1}{2L} \sum_{i=1}^n q_{1,i} \|\nabla \ell_i(w_1) - \nabla \ell_i(w_*)\|_2^2 - \frac{\mu A_1}{2} \|w_* - w_1\|_2^2 - A_1 \nu \Delta_D(q_*, q_1) \\ &\quad - \frac{a_1 \mu}{2} \|w_1 - w_*\|_2^2 - \frac{a_1 \nu}{2} \|q_1 - q_*\|_2^2, \end{aligned}$$

where the last two terms are the result of the additional quadratic slack terms in γ_1 . All of the terms from the display above will be telescoped. Thus, we apply Lem. 11 and collect the unmatched terms from the $t \geq 2$ one-step bound (using that $A_0 = 0$). The term (53) can be viewed as counting the remainder of (36) after it has telescoped some but not all terms $\frac{a_{\pi(T-1,i)}}{4L} \mathbb{E}_0 \left[q_{\pi(T-1,i)} \|\nabla \ell_i(w_{\pi(T-1,i)}) - \nabla \ell_i(w_*)\|_2^2 \right]$ across iterations. \square

C.3.5 Completing the Proof

We use similar techniques as before to bound the remaining terms from the T -step progress bound given in Lem. 13. We may now prove the main result.

Theorem 1. *Define the sequence*

$$a_1 = 1, a_2 = 4\eta, \text{ and } a_t = (1 + \eta) a_{t-1} \text{ for } t > 2,$$

along with its partial sum $A_t = \sum_{\tau=1}^t a_\tau$. There is an absolute constant C such that using the parameter

$$\eta = C \min \left\{ \frac{b}{n}, \frac{\mu}{Lnq_{\max}}, \frac{b}{n} \sqrt{\frac{\mu\nu}{nG^2}} \right\},$$

the iterates of DRAGO satisfy:

$$\sum_{t=1}^T a_t \mathbb{E}_0[\gamma_t] + \frac{A_T \mu}{4} \mathbb{E}_0 \|w_T - w_*\|_2^2 + \frac{A_T \nu}{4} \mathbb{E}_0 \|q_T - q_*\|_2^2 \leq \frac{nG^2}{\nu\mu^2} \|\nabla \ell(w_0)^\top q_0\|_2^2.$$

Proof. We first apply Lem. 13, and proceed to bound the inner product terms (51) and (52). Apply Young's inequality with parameter $\nu A_{T-1}/2$ to get

$$\begin{aligned} a_T \mathbb{E}_0 \left[(q_* - q_T)^\top (\ell(w_T) - \hat{\ell}_T) \right] &\leq \frac{\nu A_{T-1}}{4} \mathbb{E}_0 \|q_* - q_T\|_2^2 + \frac{a_T^2}{\nu A_{T-1}} \mathbb{E}_0 \|\ell(w_T) - \hat{\ell}_T\|_2^2 \\ &\leq \frac{\nu A_{T-1}}{4} \mathbb{E}_0 \|q_* - q_T\|_2^2 + \frac{a_T^2 G^2}{\nu A_{T-1}} \sum_{\tau=T-n/b}^{T-2} \mathbb{E}_0 \|w_T - w_{\tau\nu 0}\|_2^2 \\ &\leq \frac{\nu A_{T-1}}{4} \mathbb{E}_0 \|q_* - q_T\|_2^2 + \frac{a_T \alpha G^2}{\nu} \sum_{\tau=T-n/b}^{T-2} \mathbb{E}_0 \|w_T - w_{\tau\nu 0}\|_2^2. \end{aligned}$$

The left-hand term will be canceled by (57) by applying strong concavity (leaving behind $-\frac{\nu A_{T-1}}{4} \mathbb{E}_0 \|q_* - q_T\|_2^2$) and the right-hand term (because of the condition $\alpha \leq \frac{\sqrt{\mu\nu}}{4n^{3/2}G}$) will be canceled by (56). Next, consider (52). By Young's

inequality with parameter $\mu A_{T-1}/2$, we have

$$\begin{aligned}
& -a_T \mathbb{E}_0 \left[\langle \nabla \ell(w_T)^\top q_T - \hat{g}_{T-1}^\top \hat{q}_{T-1}, w_\star - w_T \rangle \right] \\
& \leq \frac{a_T^2}{\mu A_{T-1}} \mathbb{E}_0 \left\| \nabla \ell(w_T)^\top q_T - \hat{g}_{T-1}^\top \hat{q}_{T-1} \right\|_2^2 + \frac{\mu A_{T-1}}{4} \mathbb{E}_0 \|w_\star - w_T\|_2^2 \\
& \leq \frac{a_T \alpha}{\mu} \mathbb{E}_0 \left\| \nabla \ell(w_T)^\top q_T - \hat{g}_{T-1}^\top \hat{q}_{T-1} \right\|_2^2 + \frac{\mu A_{T-1}}{4} \mathbb{E}_0 \|w_\star - w_T\|_2^2,
\end{aligned}$$

where the second term will be canceled by (55). For the remaining term,

$$\begin{aligned}
& \mathbb{E}_0 \left\| \nabla \ell(w_T)^\top q_T - \hat{g}_{T-1}^\top \hat{q}_{T-1} \right\|_2^2 \\
& \leq \mathbb{E}_0 \left\| (\nabla \ell(w_T) - \ell(w_\star))^\top q_T + \nabla \ell(w_\star)^\top (q_T - \hat{q}_{T-1}) + (\nabla \ell(w_\star) - \hat{g}_{T-1})^\top \hat{q}_{T-1} \right\|_2^2 \\
& \leq 3\mathbb{E}_0 \left\| (\nabla \ell(w_T) - \nabla \ell(w_\star))^\top q_T \right\|_2^2 + 3\mathbb{E}_0 \left\| \nabla \ell(w_\star)^\top (q_T - \hat{q}_{T-1}) \right\|_2^2 + 3\mathbb{E}_0 \left\| (\nabla \ell(w_\star) - \hat{g}_{T-1})^\top \hat{q}_{T-1} \right\|_2^2 \\
& \leq 3\sigma_n \sum_{i=1}^n \mathbb{E}_0 \left[q_{T,i} \|\nabla \ell_i(w_T) - \nabla \ell_i(w_\star)\|_2^2 \right] + 3nG^2 \mathbb{E}_0 \|q_T - \hat{q}_{T-1}\|_2^2 + 3\sigma_n \sum_{i=1}^n \mathbb{E}_0 \left[\hat{q}_{T-1,i} \|\nabla \ell_i(w_\star) - \hat{g}_{T-1,i}\|_2^2 \right]
\end{aligned}$$

We may add the middle term above to (54), so that the remaining term to bound is

$$\frac{6nG^2\alpha}{\mu} \sum_{t=1}^{T+1} a_{t-1} \mathbb{E}_0 \|q_{t-1} - \hat{q}_{t-2}\|_2^2 - \sum_{t=1}^T \frac{A_{t-1}\nu}{2} \mathbb{E}_0 [\Delta_D(q_t, q_{t-1})].$$

To show that this quantity is non-negative, we use that $a_0 = 0$ and Lem. 8 (recalling that $M = n/b$ to see that

$$\frac{6nG^2\alpha}{\mu} \mathbb{E}_0 \sum_{t=1}^{T+1} a_t \|q_t - \hat{q}_{t-1}\|_2^2 \leq \frac{18e^2n^3G^2\alpha}{b^2\mu} \mathbb{E}_0 \sum_{t=1}^{T+1} a_{t-1} \|q_t - q_{t-1}\|_2^2 \leq \frac{18e^2n^3G^2\alpha^2}{b^2\mu} \mathbb{E}_0 \sum_{t=1}^T A_{t-1} \|q_t - q_{t-1}\|_2^2,$$

which will cancel with the rightmost term in (54) provided that $\alpha \leq \frac{b}{36e^2n} \sqrt{\frac{\mu\nu}{nG^2}}$. Thus, plugging the previous displays into Lem. 13, we have that

$$\begin{aligned}
\mathbb{E}_0 \left[\sum_{t=1}^T \gamma_t \right] & \leq \frac{n^2G^2}{\nu\mu^2} \left\| \nabla \ell(w_0)^\top q_0 \right\|_2^2 \\
& + \frac{3a_T\sigma_n\alpha}{2\mu} \sum_{i=1}^n \mathbb{E}_0 \left[q_{T,i} \|\nabla \ell_i(w_T) - \nabla \ell_i(w_\star)\|_2^2 \right] - \frac{a_T}{2L} \sum_{i=1}^n \mathbb{E}_0 \left[q_{T,i} \|\nabla \ell_i(w_T) - \nabla \ell_i(w_\star)\|_2^2 \right] \\
& + \frac{3\sigma_n a_T \alpha}{2\mu} \sum_{i=1}^n \mathbb{E}_0 \left[q_{\pi(T-1,i),i} \|\nabla \ell_i(w_\star) - \nabla \ell_i(w_{\pi(T-1,i)})\|_2^2 \right] \\
& - \sum_{i=1}^n (n - T + \pi(T-1,i)) \frac{a_{\pi(T-1,i)}}{4L} \mathbb{E}_0 \left[q_{\pi(T-1,i)} \|\nabla \ell_i(w_{\pi(T-1,i)}) - \nabla \ell_i(w_\star)\|_2^2 \right] \\
& - \sum_{t=1}^T \frac{a_t\mu}{4} \mathbb{E}_0 \|w_t - w_\star\|_2^2 - \sum_{t=1}^T \frac{a_t\nu}{4} \mathbb{E}_0 \|q_t - q_\star\|_2^2 \\
& - \frac{A_{T-1}\mu}{4} \mathbb{E}_0 \|w_T - w_\star\|_2^2 - \frac{A_{T-1}\nu}{4} \mathbb{E}_0 \|q_T - q_\star\|_2^2.
\end{aligned}$$

The black lines will cancel given our conditions on α . Substituting the definition of γ_t and moving the final non-positive terms on the last line, that is, $\frac{(A_{T-1}+a_T)\mu}{4} \mathbb{E}_0 \|w_T - w_\star\|_2^2$ and $\frac{(A_{T-1}+a_T)\nu}{4} \mathbb{E}_0 \|q_T - q_\star\|_2^2$ to the left-hand side achieves the claim. \square

D Implementation Details

In this section, we provide additional background on implementing DRAGO in practice. This involves a description of the algorithm amenable for direct translation into code and procedures for computing the dual proximal mapping for common ambiguity sets and penalties. We assume in this section that $\mathcal{W} = \mathbb{R}^d$ and provide multiple options for the ambiguity set \mathcal{Q} .

D.1 Algorithm Description

The full algorithm is given in Algorithm 2. We first describe the notation. Recall that $M = n/b$, or the number of blocks. We partition $[n]$ into (B_1, \dots, B_M) , where each B_K denotes a b -length list of contiguous indices. For any matrix $u \in \mathbb{R}^{n \times m}$ (including $m = 1$), we denote by $u[B_K] \in \mathbb{R}^{b \times m}$ the rows of u corresponding to the indices in B_K . Finally, for a vector $s \in \mathbb{R}^b$, we denote by se_{B_K} the vector that contains s_k in indices $k \in B_K$, and has zeros elsewhere. Next, we comment on particular aspects regarding the implementation version as compared to Algorithm 1 (Sec. 3).

- We store two versions of each table, specifically $\hat{\ell}, \hat{\ell}_1 \in \mathbb{R}^n$, $\hat{g}_1, \hat{g}_2 \in \mathbb{R}^{n \times d}$, and $\hat{q}_1, \hat{q}_2 \in \mathbb{R}^n$. For any iterate t , these variables are meant to store $\hat{\ell}_t, \hat{\ell}_{t-1} \in \mathbb{R}^n$, $\hat{g}_{t-1}, \hat{g}_{t-2} \in \mathbb{R}^{n \times d}$, and $\hat{q}_{t-1}, \hat{q}_{t-2} \in \mathbb{R}^n$.
- The quantities $\hat{g}_{\text{agg}} \in \mathbb{R}^d$ and $\hat{w}_{\text{agg}} \in \mathbb{R}^d$ are introduced as to not recompute the sums in the primal update on each iteration (which would cost $O(nd)$ operations). Instead, these aggregates are updated using $O(bd)$ operations.
- The loss and gradient tables are not updated immediately after the primal update. However, the values that fill the tables are computed, and the update occurs at the end of the loop. This is because $\hat{\ell}[B_{K_t}]$ is used to fill $\hat{\ell}_1[B_{K_t}]$ at the end of the loop, we must maintain knowledge of $\hat{\ell}[B_{K_t}]$ temporarily.
- While the proximal operator is specified for the primal in the case of $\mathcal{W} = \mathbb{R}^d$, the proximal operator for the dual is computed by a subroutine DualProx, which we describe in the next subsection.

D.2 Solving the Maximization Problem

As discussed in Appx. B, the primary examples of DRO ambiguity sets \mathcal{Q} are balls in f -divergence (specifically, KL and χ^2) and spectral risk measure sets. For the penalty D , it is also common to use f -divergences. We review these concepts in this section and provide recipes for computing the maximization problem.

f -Divergences We first recall the definition of f -divergences used throughout this section.

Definition 14. Let $f : [0, \infty) \mapsto \mathbb{R} \cup \{+\infty\}$ be a convex function such that $f(1) = 0$, $f(x)$ is finite for $x > 0$, and $\lim_{x \rightarrow 0^+} f(x) = 0$. Let q and \bar{q} be two probability mass functions defined on n atoms. The f -divergence from q to \bar{q} generated by this function f is given by

$$D_f(q \parallel \bar{q}) := \sum_{i=1}^n f\left(\frac{q_i}{\bar{q}_i}\right) \bar{q}_i,$$

where we define $0f(0/0) := 0$. For any i such that $\bar{q}_i = 0$ but $q_i > 0$, we define $D_f(q \parallel \bar{q}) := +\infty$.

The two running examples we use are the χ^2 -divergence generated by $f_{\chi^2}(x) = x^2 - 1$ and the KL divergence generated by $f_{\text{KL}}(x) = x \ln x$ on $(0, \infty)$ and define $0 \ln 0 = 0$. For any convex set $\mathcal{X} \subseteq \mathbb{R}^k$, we also introduce the convex indicator function

$$\iota_{\mathcal{X}}(x) := \begin{cases} 0 & \text{if } x \in \mathcal{X} \\ 1 & \text{otherwise} \end{cases}.$$

In either of the two cases below, we select the penalty $D(q \parallel \mathbf{1}/n) = D_f(q \parallel \mathbf{1}/n)$ to be an f -divergence. Denote in addition f^* as the Fenchel conjugate of f .

Algorithm 2 DRAGO: Implementation Version

Input: Learning rate parameter $\eta > 0$, batch size $b \in \{1, \dots, n\}$, number of iterations T .

Initialization:

$w \leftarrow 0_d$ and $q \leftarrow \mathbf{1}/n$

$\hat{\ell} \leftarrow \ell(w)$, $\hat{\ell}_1 \leftarrow \ell(w)$, $\hat{g}_1 \leftarrow \nabla \ell(w)$, $\hat{g}_2 \leftarrow \nabla \ell(w)$, $\hat{q}_1 \leftarrow q$ and $\hat{q}_2 \leftarrow q$

$\hat{w}_K \leftarrow w$ for $K \in \{1, \dots, M\}$ for $M = n/b$

$\hat{g}_{\text{agg}} \leftarrow \hat{g}_1^\top \hat{q}_1$ and $\hat{w}_{\text{agg}} \leftarrow \sum_{K=1}^M \hat{w}_K$

$\bar{\beta} = 1/[16\eta(1+\eta)(n/b-1)^2]$ if $n/b > 1$ and 0 otherwise

for $t = 1$ **to** T **do**

Sample blocks I_t and J_t uniformly on $[n/b]$ and compute $K_t = t \bmod (n/b) + 1$

$\beta_t \leftarrow (1 - (1 + \eta)^{1-t})/(\eta(1 + \eta))$

Primal Update:

$g \leftarrow [\nabla \ell_i(w)]_{i \in B_{I_t}} \in \mathbb{R}^{b \times d}$ and $v^P \leftarrow \hat{g}_{\text{agg}} + \frac{1}{1+\eta} \delta^P$.

$w \leftarrow \frac{1}{(1+\beta_t)} ((\beta_t - \bar{\beta}(M-1))w + \bar{\beta}(\hat{w}_{\text{agg}} - \hat{w}_{K_t}) - v^P/\mu)$

$\hat{w}_{\text{agg}} \leftarrow \hat{w}_{\text{agg}} + w - \hat{w}_{K_t}$ and $\hat{w}_{K_t} \leftarrow w$

Compute Loss and Gradient Table Updates:

$(l_t, g_t) \leftarrow [\ell_k(w), \nabla \ell_k(w)]_{k \in B_{K_t}} \in \mathbb{R}^b \times \mathbb{R}^{b \times d}$

Dual Update:

$l \leftarrow [\ell_j(w)]_{j \in B_{J_t}} \in \mathbb{R}^b$

$\delta^D \leftarrow M(l - \hat{\ell}_1[J_t])$ and $v^D \leftarrow \hat{\ell} + (l - \hat{\ell}[B_{K_t}])e_{B_{K_t}} + \frac{1}{1+\eta} \delta^D e_{B_{J_t}}$

$q \leftarrow \text{DualProx}(q, v^D, \beta_t) = \arg \max_{\bar{q} \in \mathcal{Q}} \{ \langle v^D, \bar{q} \rangle - \nu D(\bar{q} \| \mathbf{1}_n/n) - \beta_t \nu \Delta_D(\bar{q}, q) \}$

Update All Tables:

$\hat{g}_2[B_{K_t}] \leftarrow \hat{g}_1[B_{K_t}]$ and $\hat{g}_1[B_{K_t}] \leftarrow g_t$

$\hat{\ell}_1[B_{K_t}] \leftarrow \hat{\ell}[B_{K_t}]$ and $\hat{\ell}[B_{K_t}] \leftarrow l_t$

$\hat{q}_2[B_{K_t}] \leftarrow \hat{q}_1[B_{K_t}]$ and $\hat{q}_1[B_{K_t}] \leftarrow q[B_{K_t}]$

$\hat{g}_{\text{agg}} \leftarrow \hat{g}_{\text{agg}} + \hat{g}_1[B_{K_t}]^\top \hat{q}_1[B_{K_t}] - \hat{g}_2[B_{K_t}]^\top \hat{q}_2[B_{K_t}]$

end for

return (w, q) .

D.2.1 Spectral Risk Measure Ambiguity Sets

As in Appx. B, the spectral risk measure ambiguity set is defined by a set of non-decreasing, non-negative weights $\sigma = (\sigma_1, \dots, \sigma_n)$ that sum to one. Our ambiguity set is given by

$$\mathcal{Q} = \mathcal{Q}(\sigma) := \text{conv}(\{\text{permutations of } \sigma\}),$$

and we use D_f has the penalty for either f_{χ^2} or f_{KL} . The set $\mathcal{Q}(\sigma)$ is referred to the *permutahedron* on σ . In this case, the maximization problem can be dualized and solved via the following result.

Proposition 15. (Mehta et al., 2024, Proposition 3) *Let $l \in \mathbb{R}^n$ be a vector and π be a permutation that sorts its entries in non-decreasing order; i.e., $l_{\pi(1)} \leq \dots \leq l_{\pi(n)}$. Consider a function f strictly convex with strictly convex conjugate defining a divergence D_f . Then, the maximization over the permutahedron subject to the shift penalty can be expressed as*

$$\max_{q \in \mathcal{Q}(\sigma)} \{q^\top l - \nu D_f(q \| \mathbf{1}_n/n)\} = \min_{\substack{z \in \mathbb{R}^n \\ z_1 \leq \dots \leq z_n}} \sum_{i=1}^n g_i(z; l), \quad (59)$$

where we define $g_i(z; l) := \sigma_i z + \frac{\nu}{n} f^* \left((l_{\pi(i)} - z)/\nu \right)$. The optima of both problems, denoted

$$z^{\text{opt}}(l) = \arg \min_{\substack{z \in \mathbb{R}^n \\ z_1 \leq \dots \leq z_n}} \sum_{i=1}^n g_i(z; l), \quad q^{\text{opt}} = \arg \max_{q \in \mathcal{Q}(\sigma)} q^\top l - \nu D_f(q \| \mathbf{1}_n/n),$$

are related as $q^{\text{opt}}(l) = \nabla(\nu D_f(\cdot \| \mathbf{1}_n/n))^*(l - z_{\pi^{-1}}^{\text{opt}}(l))$, that is,

$$q_i^{\text{opt}}(l) = \frac{1}{n} [f^*]^\prime \left(\frac{1}{\nu} (l_i - z_{\pi^{-1}(i)}^{\text{opt}}(l)) \right). \quad (60)$$

As described in [Mehta et al. \(2024, Appendix C\)](#), the minimization problem (59) is an exact instance of isotonic regression and can be solved efficiently with the pool adjacent violators (PAV) algorithm.

D.2.2 Divergence-Ball Ambiguity Sets

Another common ambiguity set format is a ball in f -divergence, or

$$\mathcal{Q} = \mathcal{Q}(\rho) := \{q \in \mathbb{R}^n : D_f(q \| \mathbf{1}/n) \leq \rho, q \geq 0, \text{ and } \mathbf{1}^\top q = 1\}.$$

We describe the case of the rescaled χ^2 -divergence in particular, in which the feasible set is an ℓ_2 -ball intersected with the probability simplex. Given a vector $l \in \mathbb{R}^n$, we aim to compute the mapping

$$l \mapsto \arg \max_{\substack{q \in \mathcal{P}_n \\ \frac{1}{2} \|q - \mathbf{1}/n\|_2^2 \leq \rho}} \langle l, q \rangle - \frac{\nu}{2} \|q - \mathbf{1}/n\|_2^2, \quad (61)$$

where $\mathcal{P}_n := \{q \in \mathbb{R}^n : q \geq 0, \mathbf{1}^\top q = 1\}$ denotes the n -dimensional probability simplex. We apply a similar approach to [Namkoong and Duchi \(2017\)](#), in which we take a partial dual of the problem above. Indeed, note first that for any $q \in \mathcal{P}_n$, we have that $\frac{1}{2} \|q - \mathbf{1}_n/n\|_2^2 = \frac{1}{2} \|q\|_2^2 - \frac{1}{2n}$. Thus, the optimal solution to (61) can be computed by solving

$$\max_{q \in \mathcal{P}_n} \min_{\lambda \geq 0} \langle l, q \rangle - \frac{\nu}{2} \|q\|_2^2 - \lambda \left(\frac{1}{2} \|q\|_2^2 - \rho - \frac{1}{2n} \right),$$

or equivalently, by strong duality via Slater's condition, solving

$$\max_{\lambda \geq 0} \left[f(\lambda) := (\nu + \lambda) \min_{q \in \mathcal{P}_n} \frac{1}{2} \|q - l/(\nu + \lambda)\|_2^2 - \lambda \left(\rho + \frac{1}{2n} \right) - \frac{1}{2(\nu + \lambda)} \|l\|_2^2 \right].$$

Notice that evaluation of the outer objective itself requires Euclidean projection onto the probability simplex as a subroutine, after which the maximization problem can be computed via the bisection method, as it is a univariate concave maximization problem over a convex set. In order to determine which half to remove in the bisection search, we also compute the derivative of $\lambda \mapsto f(\lambda)$, which is given by

$$f'(\lambda) := \frac{1}{2} \|q^{\text{opt}}(\lambda)\|_2^2 - \rho - \frac{1}{2n},$$

where $q^{\text{opt}}(\lambda)$ achieves the minimum in $\min_{q \in \mathcal{P}_n} \frac{1}{2} \|q - l/(\nu + \lambda)\|_2^2$ for a fixed $\lambda \geq 0$. For projection onto the probability simplex, we apply Algorithm 1 from [Condat \(2016\)](#), which is a solution relying on sorting the projected vector. The overall method consists of three steps.

1. **Sorting:** Projection onto the simplex relies on sorting the vector $l/(\nu + \lambda)$ on each evaluation. However, because $l/(\nu + \lambda)$ varies from evaluation to evaluation simply by multiplying by a positive scalar, we may pre-sort l and use the same sorted indices on each evaluation of $(f(\lambda), f'(\lambda))$ listed below.
2. **Two-Pointer Search:** We find the upper and lower limits for λ by initializing $\lambda_{\min} = 0$ and $\lambda_{\max} = 1$, and repeatedly making the replacement $(\lambda_{\min}, \lambda_{\max}) \leftarrow (\lambda_{\max}, 2\lambda_{\max})$ until $f'(\lambda_{\max}) < -\varepsilon$ for some tolerance

$\varepsilon > 0$. This, along with $f'(\lambda_{\min}) > \varepsilon$ indicates that the optimal value of λ lies within $(\lambda_{\min}, \lambda_{\max})$. For any λ with $|f'(\lambda)| < \varepsilon$, we return the associated $q^{\text{opt}}(\lambda)$ as the solution.

3. **Binary Search:** Finally, we repeatedly evaluate $f'(\lambda)$ for $\lambda = (\lambda_{\min} + \lambda_{\max})/2$. If $f'(\lambda) > \varepsilon$, we set $\lambda_{\min} \leftarrow \lambda$, whereas if $f'(\lambda) < -\varepsilon$, then we set $\lambda_{\max} \leftarrow \lambda$. We terminate when $\lambda_{\max} - \lambda_{\min} < \varepsilon$ or $|f'(\lambda)| < \varepsilon$.

The parameter ε is set to 10^{-10} in our experiments. Note that the same procedure can be used to compute the dual proximal operator in Algorithm 1. In particular, when $\Delta_D((, q), q_{t-1}) = \frac{1}{2} \|q - q_t\|_2^2$, which is true when D is the χ^2 -divergence, then

$$q_t = \arg \max_{\substack{q \in \mathcal{P}_n \\ \frac{1}{2} \|q - \mathbf{1}/n\|_2^2 \leq \frac{\rho}{n}}} \langle l + \nu \beta_t q_t, q \rangle - \frac{\nu(1 + \beta_t)}{2} \|q - \mathbf{1}/n\|_2^2,$$

which is a particular case of (61), and hence can be solved using the exact same procedure. The runtime of this subroutine is $O(n \log n + n \log(1/\varepsilon))$, accounting for both the initial sorting at $O(n \log n)$ cost, and the $O(\log(1/\varepsilon))$ iterations of the exponential and binary searches. Each iteration requires a linear scan of n elements at cost $O(n)$.

Hardware Acceleration Finally, note that the computations in Appx. D.2 and Appx. D.2.2 involve primitives such as sorting, linear scanning through vectors, and binary search. Due to their serial nature (as opposed to algorithms that rely on highly parallelizable operations such as matrix multiplication), we also utilize just-in-time compilation on the CPU via the Numba package for increased efficiency.

Dataset	d	n	Task	Source
yacht	6	244	Regression	UCI
energy	8	614	Regression	UCI
concrete	8	824	Regression	UCI
kin8nm	8	6,553	Regression	OpenML
power	4	7,654	Regression	UCI
acsincome	202	4,000	Regression	Fairlearn
emotion	270	8,000	Multiclass Classification	Hugging Face

Table 5: Dataset attributes such as sample size n , parameter dimension d , and sources.

E Experimental Details

We describe details of the experimental setup, including datasets, compute environment, and hyperparameter tuning. We largely maintain the benchmarks of [Mehta et al. \(2023\)](#).

E.1 Datasets

The sample sizes, dimensions, and source of the datasets are summarized in Tab. 5. The tasks associated with each dataset are listed below.

- (a) *yacht*: predicting the residuary resistance of a sailing yacht based on its physical attributes [Tsanas and Xifara \(2012\)](#).
- (b) *energy*: predicting the cooling load of a building based on its physical attributes [Baressi Segota et al. \(2020\)](#).
- (c) *concrete*: predicting the compressive strength of a concrete type based on its physical and chemical attributes [Yeh \(2006\)](#).
- (d) *kin8nm*: predicting the distance of an 8 link all-revolute robot arm to a spatial endpoint ([Akujuobi and Zhang, 2017](#)).
- (e) *power*: predicting net hourly electrical energy output of a power plant given environmental factors ([Tüfekci, 2014](#)).
- (f) *acsincome*: predicting income of US adults given features compiled from the American Community Survey (ACS) Public Use Microdata Sample (PUMS) ([Ding et al., 2021](#)).
- (g) *emotion*: predicting the sentiment of sentence in the form of six emotions. Each input is a segment of text and we use a BERT neural network [Devlin et al. \(2019\)](#) as an initial feature map. This representation is fine-tuned using 2 epochs on a random half (8,000 examples) of the original emotion dataset, and then applied to the remaining half. We then apply principle components analysis (PCA) to reduce the dimension of each vector to 45.

E.2 Hyperparameter Selection

We fix a minibatch size of 64 SGD and an epoch length of $N = n$ for LSVRG. In practice, the regularization parameter μ and shift cost ν are tuned by a statistical metric, i.e. generalization error as measured on a validation set.

For the tuned hyperparameters, we use the following method. Let $k \in \{1, \dots, K\}$ be a seed that determines algorithmic randomness. This corresponds to sampling a minibatch without replacement for SGD and SRDA and a single sampled index for LSVRG. Letting $\mathcal{L}_k(\eta)$ denote the average value of the training loss of the last ten passes using learning rate η and seed k , the quantity $\mathcal{L}(\eta) = \frac{1}{K} \sum_{k=1}^K \mathcal{L}_k(\eta)$ was minimized to select η . The learning rate η is chosen in the set $\{1 \times 10^{-4}, 3 \times 10^{-4}, 1 \times 10^{-3}, 3 \times 10^{-3}, 1 \times 10^{-2}, 3 \times 10^{-2}, 1 \times 10^{-1}, 3 \times 10^{-1}, 1 \times 10^0, 3 \times 10^0\}$, with two orders of magnitude lower numbers used in *acsincome* due to its sparsity. We discard any learning rates that cause the optimizer to diverge for any seed.

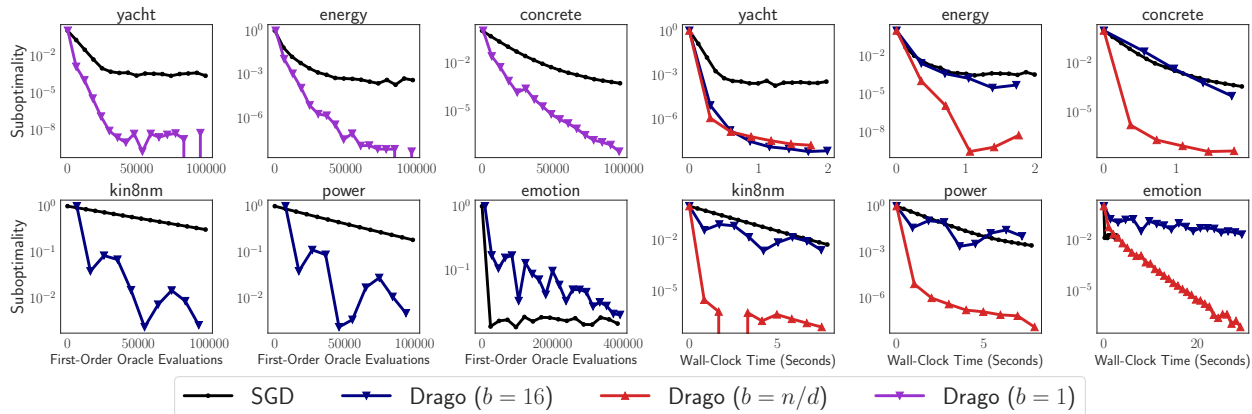


Figure 4: **Benchmarks on the χ^2 Ambiguity Set.** In both panels, the y -axis measure the primal suboptimality gap, defined in (11). Individual plots correspond to particular datasets. **Left:** The x -axis displays the number of individual first-order oracle queries to $\{(\ell_i, \nabla \ell_i)\}_{i=1}^n$. **Right:** The x -axis displays wall-clock time.

E.3 Compute Environment

Experiments were run on a CPU workstation with an Intel i9 processor, a clock speed of 2.80GHz, 32 virtual cores, and 126G of memory. The code used in this project was written in Python 3 using the Numba packages for just-in-time compilation. Run-time experiments were conducted without CPU parallelism. The algorithms are primarily written in PyTorch and support automatic differentiation.

E.4 Additional Experiments

In Sec. 4, we mainly show performance on spectral risk-based ambiguity sets, in particular the conditional value-at-risk (CVaR). In this section, we also consider f -divergence ball-based ambiguity sets, with the procedure described in Appx. D.2.2. As in Namkoong and Duchi (2017), we use a radius that is inversely proportional to the sample size, namely $\rho = \frac{1}{n}$, and the strong convexity-strong concavity parameter $\mu = \nu = 1$. In Fig. 4, we demonstrate the performance of DRAGO with $b = 1$, $b = 16$ (as chosen heuristically), and $b = n/d$. We compare against the biased stochastic gradient descent, which can be defined using oracle to compute the optimal dual variables given a vector of losses; however, note that LSVRG is designed only for spectral risk measures, so the method does not apply in the divergence ball setting. We observe that the optimization performance across both regression and multi-class classification tasks are qualitatively similar to that seen in Fig. 2 and Fig. 3. The $b = 1$ variant performs well on smaller datasets ($n \leq 1,000$), whereas the $b = 16$ heuristic generally does not dominate in terms of gradient evaluations or wall time. While the number of gradient evaluations is significantly larger for the $b = n/d$ variant, implementation techniques such as just-in-time compilation (see Appx. D) allow for efficient computation, resulting in better overall optimization performance as a function of wall time.